

1 **TOWARDS A MORE ROBUST REPRESENTATION OF LITHIC INDUSTRIES**
2 **IN ARCHAEOLOGY: A CRITICAL REVIEW OF TRADITIONAL**
3 **APPROACHES AND MODERN TECHNIQUES**

4
5 Julien Looten¹, Brad Gravina^{2,3}, Xavier Muth^{4,5}, Maxime Villaeys², Jean-Guillaume
6 Bordes³

7 ¹ University of Lille, UMR-8164 HALMA, Lille, France

8 ² Musée national de Préhistoire, Les Eyzies, France

9 ³ University of Bordeaux, UMR-5199 PACEA, Bordeaux, France

10 ⁴ Get in Situ, Riex, Switzerland

11 ⁵ School of Engineering and Management Vaud, HES-SO University of Applied Sciences
12 and Arts Western Switzerland

13

14 *Corresponding author

15 Correspondence: j.looten62@gmail.com

16

17 **ABSTRACT**

18 Often comprising vast numbers of artifacts, prehistoric lithic assemblages are
19 presented in publications in the form of drawings, diagrams, photographs, or extracts
20 from 3D acquisitions. These visual representations are designed to highlight the most
21 characteristic typological and technological features of a given assemblage. However,
22 the selection of pieces to illustrate is dictated by constraints of time, budget, or space.
23 Moreover, inaccuracies in drawings or poorly lit photographs can cause confusion and
24 problems of interpretation, while more precise, complex, or time-consuming methods
25 can only be applied to a limited number of objects.

26 After a brief overview of the advantages and limitations of the main types of
27 stone tool representations, namely standard drawing and photography, we detail the
28 acquisition of 3D models through photogrammetry in relation to Reflectance
29 Transformation Imaging (RTI). Although less widely known than 3D imaging, RTI is an
30 inexpensive, easily transferred photographic method that can be performed using non-
31 specialist equipment. It allows for the visualization of an object's interactions with
32 artificial light and enhances the perception of its microtopography. RTI provides a more
33 comprehensive documentation of stone tools, including flake scars, use-wear traces,
34 and post-depositional alterations, and thereby enhances the accuracy and, by
35 extension, the objectivity of stone tool representations and artifact characterization.

36

37 **Keywords:** Stone tools, lithic artefacts, representation, RTI (Reflectance
38 Transformation Imaging), photography, 3D models, photogrammetry, modern
39 techniques, prehistory

1. Introduction: The challenge of presenting lithic artifacts

41 Prehistoric lithic industries are typically composed of thousands, or even tens of
42 thousands, of artifacts of all sizes, making it impossible to visually represent all pieces in
43 publications. While count tables help describe these large populations of objects, the
44 typological and technological definitions of the categories used to produce these counts are
45 not universally shared. Consequently, the visual representation of artifacts plays a
46 significant role in supporting the description and interpretation of stone tool assemblages.
47 This illustrated subset often depicts only a very small numerical portion of the entire
48 collection and is carefully selected to support a specific argument; it is therefore
49 unrepresentative of the assemblage as a whole.

50

51 Moreover, the number of artifacts represented depends on the publication medium, as
52 well as budgetary and time constraints associated with producing the illustrations. While the
53 ideal scenario would be to represent all the artifacts in a collection, giving readers the best
54 opportunity to assess the coherency between the descriptions provided, the interpretations
55 proposed, and the physical reality of each object, this is rarely ever fully achieved.
56 Nevertheless, making the largest possible number of artifacts accessible, appreciable, and
57 manipulable for the scientific community enhances the robustness of the data through
58 greater transparency of the criteria underlying interpretations. Striving toward this objective
59 is not limited to research alone; it also extends to higher education and broader public
60 dissemination.

61

62 In addition to drawings, the traditional form of representing prehistoric lithic industries,
63 new visual techniques, such as photography, three-dimensional scanning, and
64 photogrammetry, represent significant technological advances in presenting artifacts in
65 publications.

66

67 After briefly reviewing the advantages and limitations of these various approaches, we
68 argue that a photographic method, rarely applied to lithic industries, Reflectance
69 Transformation Imaging (RTI), presents a means of producing high-fidelity reproductions of
70 objects while being easy to implement for a large number of artifacts

71

72

2. Traditional representation: drawing stone tools

73 From the moment ancient stone tools were first recognized, their graphic representation
74 emerged as the preferred visualization tool, serving alongside written descriptions as proof
75 of the intentional nature of their manufacture or their association with a particular civilization
76 or epoch. Early drawings of stone tools (Fig. 1) played a crucial role in the history of
77 Prehistory, particularly demonstrating the deep antiquity of human-made tools. The effort to
78 codify and standardize the graphic representation of stone tools began to emerge as early
79 as the beginning of the 19th century. "Enhancing hatching" was used to illustrate removals
80 and the relief of each piece, although these early hatching techniques differed from those
81 used today. Their placement and extent were then more freely applied in the absence of
82 strict standards (Fig. 2).

83

84

85

86

87

88

89

90

91

92

93

94

95

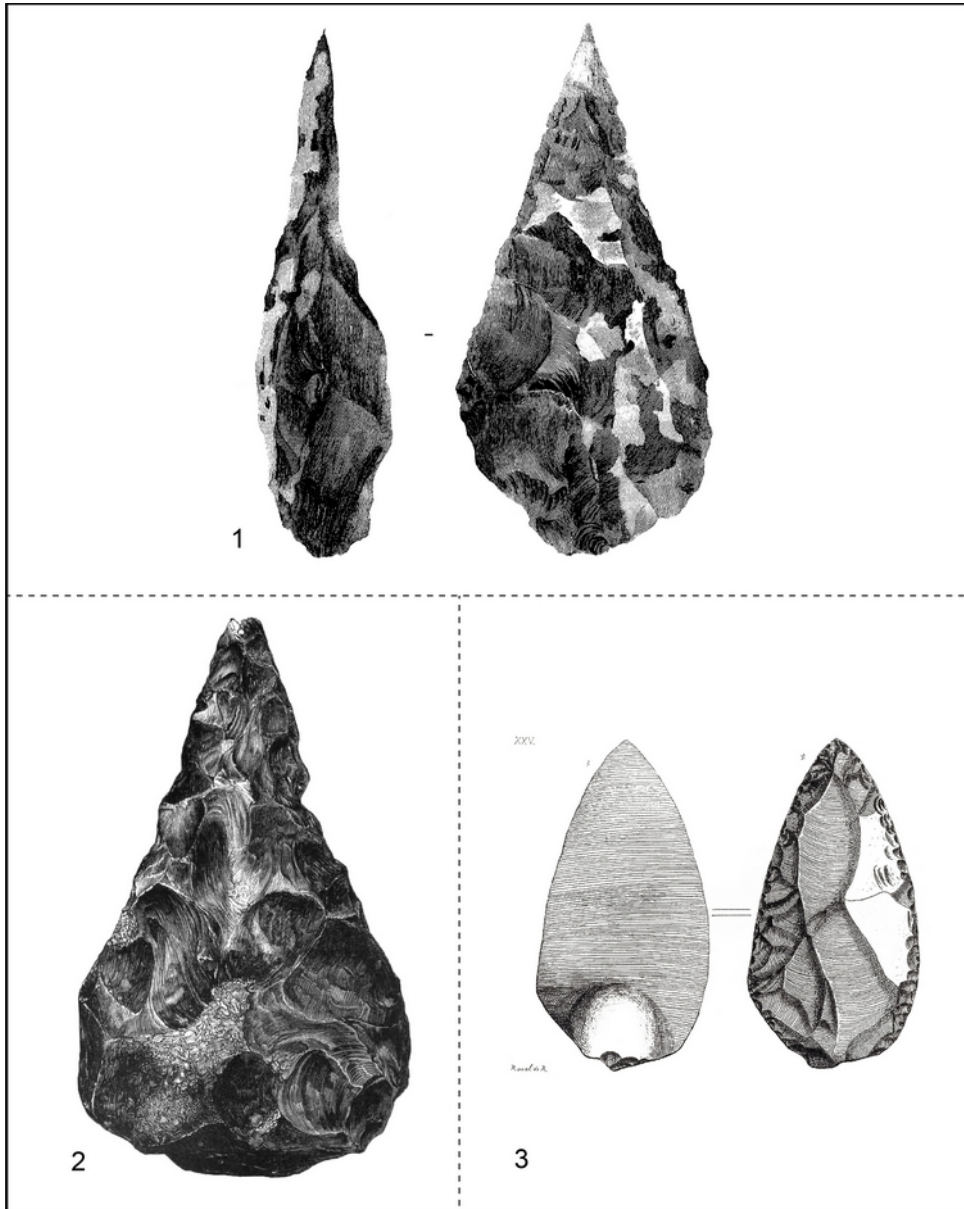
96

97

98

99

100



101

Figure 1 - Historical illustrations of paleolithic lithic artifacts

102

1. Drawing of a handaxe from Hoxne (Suffolk, England), published by John Frere in 1800 in *Archaeologia* (Frere, 1800, pl.15). In this letter, J. Frere concluded that these artifacts were "weapons of war, fabricated by a people who had not the use of metals" and that "the situation in which these weapons were found may tempt us to refer them to a very remote period indeed: even beyond that of the present world"—one of the earliest hypotheses advocating for the antiquity of humanity, foreshadowing the later recognition of what would be called Prehistory. It would take more than 50

109

110

111

112

113

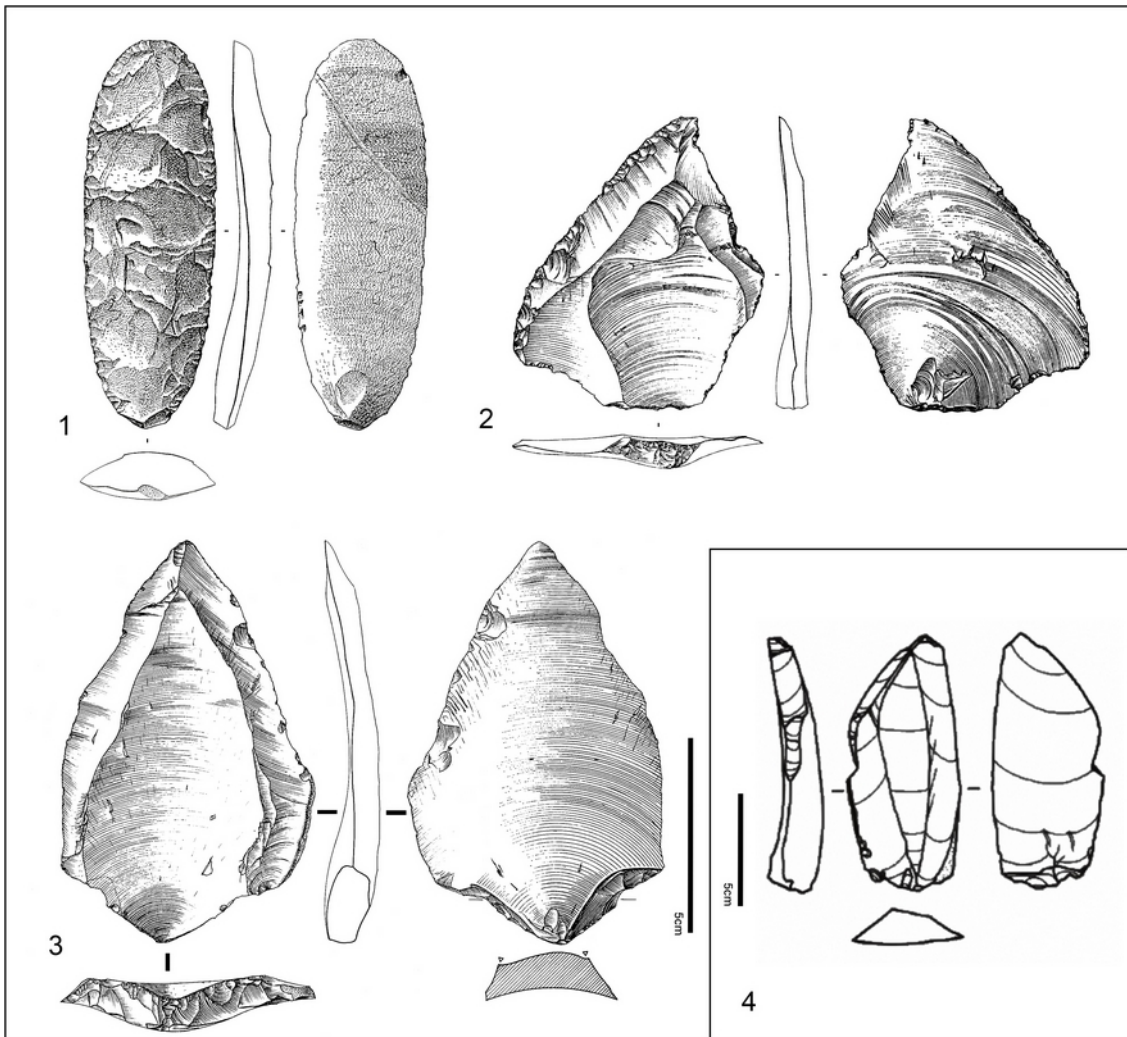
114

115

116

years for John Evans to reconsider J. Frere's observations. **2.** Representation of a handaxe discovered at Gray's Inn Lane (London, England), extracted from *The Ancient Stone Implements, Weapons and Ornaments of Great Britain* by John Evans (Evans, 1872, pl. 451, p. 522). **3.** Illustration of a convergent double scraper from the Grotte des Cottés (Vienne, France), drawn by Raoul de Rochebrune (Rochebrune, 1881).

117 The desire to standardize the descriptive characteristics for classifying these
 118 assemblages of artifacts quickly led to the adoption of technical drawing conventions (Fig.
 119 2). These conventions, adapted to the specificities of hard stones, remain widely used in
 120 scientific publications today (Dauvois, 1976; Laurent, 1985; Addington, 1986; Martingell &
 121 Saville, 1988; Assié, 1995; Inizan *et al.*, 1995; Cauche, 2020 ; [Cerasoni, 2021](#) ; [Timbrell, 2022](#)).
 122 Within the international community of lithic specialists are generally familiar with
 123 “enhancement hatching” and how to interpret it to better reconstruct the stages of an
 124 object's manufacture, with some countries adopting specific standards, such as Japan (Fig.
 125 2, no.4).
 126



128 **Figure 2 – 1 to 3.** Traditional drawings (Dauvois, 1976, modified). A.
 129 Gossolorum, Ténéré (Niger), quartzite scraper. B. Abou-Sif (Jordan),
 130 Levallois flake scraper in flint. C. Carrière Bervialle I, Les Hautes-Bruyères
 131 (Hauts-de-Seine, France), Levallois point in flint. **4.** Specific drawing
 132 standards, the example of Japan - Hirosato-type microblade cores
 133 (Hokkaido, Northern Japan ; Takakura, 2020).

134
 135

136

137 The evolution of drawing practices has mirrored advancements in investigative methods
138 for lithic industries. Initially artistic and qualitative—where an industry was often
139 characterized by a few “diagnostic fossils”—it became increasingly technical and precise
140 with the advent of statistical typology (Bordes, 1953). This shift led to the creation of an
141 ever-growing number of drawing plates, extending beyond the main shaped or retouched
142 pieces to equally reflect their relative proportions (e.g., Sonnevile-Bordes, 1960). More
143 recently, the widespread adoption of the techno-economic approach has resulted in the
144 inclusion of a broader range of artefact categories deemed significant. Thus, cores,
145 knapping accidents, and unmodified products have become increasingly common in
146 drawing plates. These have been supplanted by diacritical sketches, focusing on object
147 manufacturing methods, which are often less demanding to execute than traditional
148 drawings (Fig. 3).

149

150 Traditional lithic drawing, characterized by hatching, presents several drawbacks:

151

152 - The production of lithic artifact drawings requires not only significant time but also
153 varies greatly between artifact types. A survey of four experienced illustrators (Jacques
154 Jaubert, Gauthier Devilder, Nelson Ahmed-Delacroix, and Celia Fatcheung) revealed
155 that the average time required to draw a lithic artifact ranges from 25 minutes to 8
156 hours. This wide range can be explained by factors such as the number of views and
157 removals, as well as the type of raw material. One of the surveyed illustrators
158 highlighted this variability with two extreme examples. In the first case, drawing an
159 unretouched flint blade — featuring a top view, a schematic profile view, and a view of
160 the butt — can be completed in 20 minutes, including the measurement of the piece
161 and digital grayscale processing before publication. In contrast, drawing a phonolite
162 biface requiring six detailed views can take between 2 to 4 hours per view, amounting
163 to over 12 hours of work for the final publication-ready illustration.

164

165 - It requires the meticulous mastery of drawing techniques, leading to highly variable
166 quality depending on the illustrator.

167

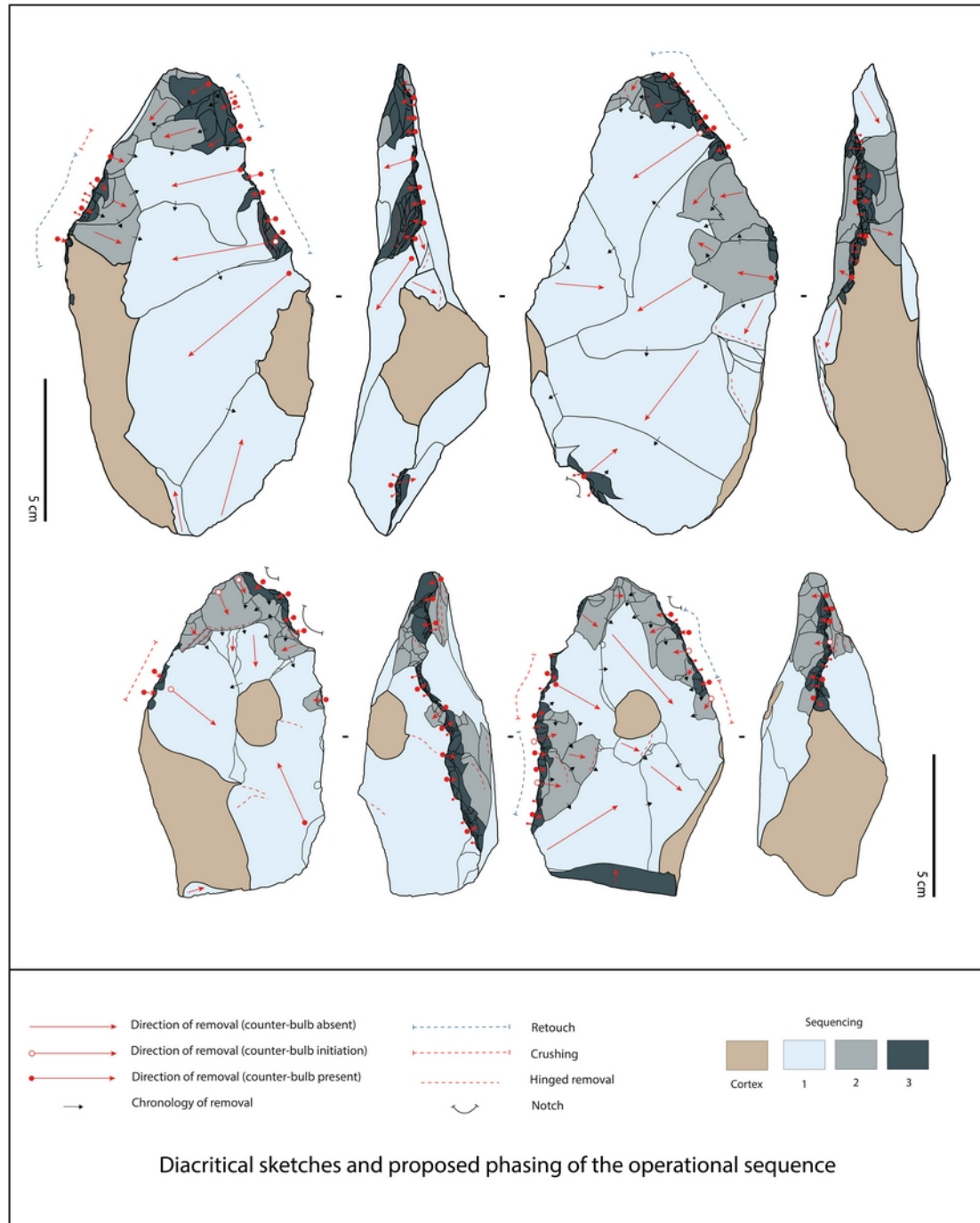
168 - It is prone to errors due to misinterpretations of technological features by the illustrator
169 and remains incomplete, as it is particularly difficult to graphically represent very small
170 removals or surface alterations. Drawing is inherently interpretative: Michel Dauvois
171 opined that "the tool is a raw fact, its drawing a scientific fact, because the object
172 precedes its understanding; between the two lies the interpretation of observation. The
173 drawing thus represents the observer's position relative to the tool" (Dauvois, 1976, p.
174 14). In other words, the drawing does not seek to reproduce every detail of an object
175 but rather tacitly illustrates a specific argument. This interpretative element may lead to
176 the intentional (or unconscious) omission of certain elements or, conversely, an
177 emphasis on others. Thus, while drawings help guide the reader in understanding a
178 given hypothesis or interpretation, it is crucial that the reader has a means of forming
179 their own opinions about the material.

180

181 Despite these shortcomings, drawing remains the foundation for defining numerous
182 categories of retouched or shaped pieces (Bordes 1961, Demars & Laurent, 1989),
183 technical pieces, or knapping accidents (Inizan *et al.*, 1995), and even techno-complexes.
184 These "types" serve as a more or less conscious reference for describing stone tool
185 industries (Bordes, 1984). Drawings remain the predominant mode of representation in

186 current publications, although they are increasingly supplemented or even replaced by
187 photographic and digital imaging methods.

188



189
190
191
192
193

Figure 3 - Diacritical sketches of two bifacial pieces from the site of Cagny l'Épinette (Somme, France). Sketches produced as part of an ongoing doctoral thesis by J. Looten, under the supervision of A. Lamotte (HALMA – UMR 8164) and co-supervised by J. Jaubert (PACEA – UMR 5199).

3. Modern practices in the digital era

195 Over the past two decades, digital imaging has become a key tool in reducing
196 interpretative biases by enabling a more objective characterization of artifacts. In this
197 section below, we present the main imaging approaches for presenting stone tools that
198 contribute to improving our understanding of the studied remains: traditional photography,
199 3D modeling, and RTI (Reflectance Transformation Imaging). These techniques are now
200 widely used, and a comprehensive overview of these methods was published by Brecko &
201 Mathys in 2020 as part of a handbook for best practices and standardization for the mass
202 digitization of natural history science collections (Brecko & Mathys, 2020)

203 3.1. Photography

204 With the advent of digital photography, photographs now often, but not always,
205 accompany drawings of stone tool industries. Easy to implement, artefact photos give the
206 impression of a faithful and objective reproduction of a material reality. The rise of online
207 publications and supplementary information has further contributed to the widespread
208 adoption of photography, as printed media offer fewer opportunities for extensive color
209 plates. This trend has accelerated with digital technology, facilitating the rapid capture of
210 high-quality, publishable images. Photography can yield valuable results, particularly in
211 rendering relief, which, under specific lighting conditions, can convey surface alterations
212 and material properties (Laurent, 1985). High-quality photographs can even reveal the
213 grain and, in some cases, the petrographic nature of knapped stones.

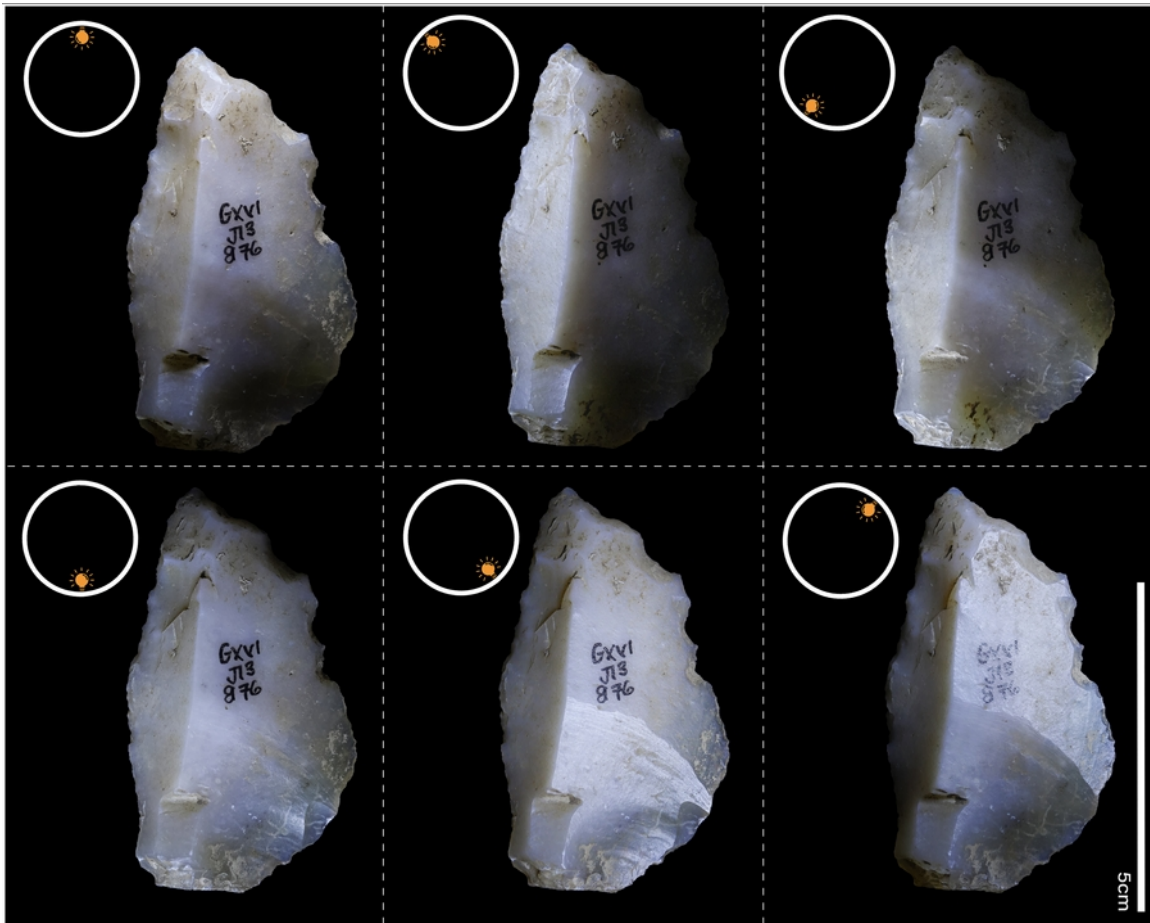
214
215 However, in practice, photographs often fail to meet expectations because they are not
216 produced under optimal conditions or with appropriate equipment. Poor lighting frequently
217 renders photos less “interpretable” compared to drawings (Fig. 4), as no single view can
218 effectively highlight all aspects of an artifact without sophisticated lighting setups and
219 sometimes hours of adjustment (Fig. 5). **Unlike 3D models, 2D photography often presents
220 optical distortions that can affect the accuracy of the representation of an archaeological
221 object. These deformations are caused by several factors, mainly optical and geometrical
222 misalignment or deformation of the sensor.**

223
224 In this context, several methods are employed to enhance artifact restitution, with
225 lighting being the key parameter. Instead of relying on a single light source (artificial or
226 natural) positioned to the upper left of the object, as convention dictates, it is possible to
227 manually determine the optimal lighting for each object using at least two or three
228 adjustable light sources (e.g., LED lights). Results vary depending on the shape
229 (particularly the thickness), but, most importantly, on the material from which the object is
230 made (e.g., translucent obsidian or highly reflective white patinas). This approach
231 nevertheless helps capture the shadows of the numerous facets of the artifacts. The
232 flexibility of movable light sources facilitates optimal positioning for low-angle lighting while
233 also allowing adjustments to the intensity of lights and shadows according to the different
234 forms and textures of artifacts.

235
236 **When photographing objects with a thickness that is too high relative to their surface
237 area, the operator quickly encounters a shallow depth of field, which directly impacts.** To
238 address this, focus stacking is commonly used. This method involves combining multiple
239 images in which the focal plane position varies along the optical axis, generating a final
240 image with an extended depth of field. The first step in focus stacking consists of capturing

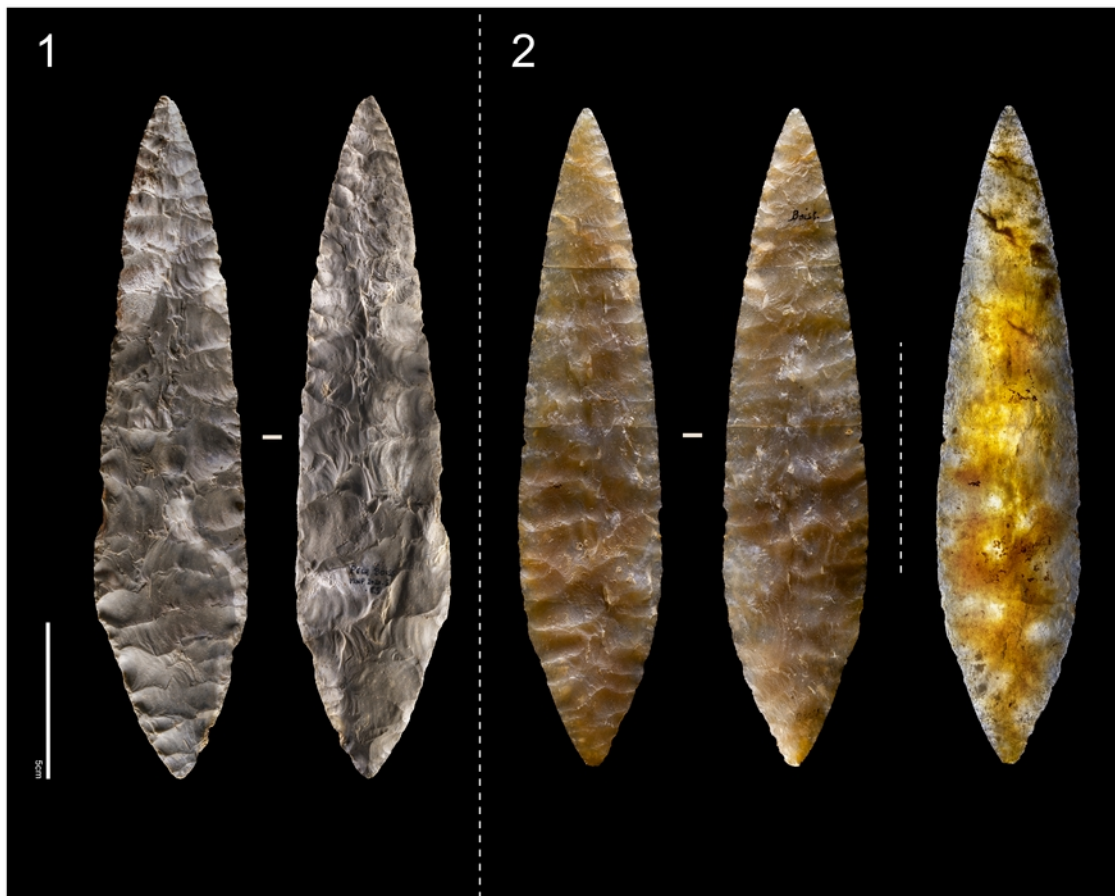
241 a series of images, each with a slightly different focal plane. This can be achieved either by
242 adjusting the focus directly or by physically shifting the camera while maintaining a fixed
243 focus setting. The second step involves digitally “stacking” the obtained images, prioritizing
244 the sharpest areas. The selection and compilation of these zones can be performed
245 manually or automatically using image-processing software. Several commercial software
246 solutions (Zerene Stacker®, CombineZP®, Helicon Focus®, and Auto-Montage®), as well
247 as open-source alternatives (such as the Focus-Stack solution available on GitHub®,
248 Forster *et al.*, 2004), enable the automatic processing of these image stacks. These
249 methods are continuously evolving, with an overview provided by Brecko *et al.* (Brecko *et*
250 *al.*, 2014).

251
252
253



255
256
257

Figure 4 - Differing perceptions of the same object depending on the angle of incidence of the lighting. Settings : Canon 6D Mark II camera – Canon 50mm f/1.8 lens – f/10 – 1/20 sec – ISO 100.



259 **Figure 5** - Photographs of two laurel leaf points from the Solutrean site of
 260 Pech de la Boissière (Dordogne, France). **1.** Image with multidirectional
 261 lighting – Captured with a Nikon D850 and a Sigma ART 50mm f/1.4 lens,
 262 settings: ISO 100, 0.5s, f/10. **2.** left: Photograph taken with multidirectional
 263 lighting – Nikon D850 and Sigma ART 50mm f/1.4, settings: ISO 100, 1.3s,
 264 f/10. Right: Photograph taken with backlighting, enhancing the transparency
 265 of the artifact – Nikon D850 and Sigma ART 50mm f/1.4, settings: ISO 100,
 266 1/160s, f/10.

267

268 **3.2. Specific Treatments**

269 Before the advent of 3D and RTI approaches, photographs were generally
 270 unsatisfactory from a technical standpoint, particularly in terms of the order and
 271 organization of removals, except in rare cases. As a result, alternative treatments were
 272 attempted to enhance visualization. For example, to improve the quality of his photographs,
 273 Jean Airvaux (Airvaux, 2005) applied multiple layers of a white crack detector spray to the
 274 surface of artifacts, while Jacques Pelegrin (Pelegrin, 2000) used magnesium powder.
 275 These methods proved effective in highlighting the relief of knapping scars, although they
 276 obscured details related the raw material. However, the direct application of substances on
 277 lithic surfaces has raised concerns among museum curators and archaeologists.

278 3.3. 3D Acquisition methods

279 Widely used for over at least a decade, 3D modeling has become a common solution
280 for illustrating and analyzing lithic objects, regardless of the acquisition method chosen. In
281 some cases, these models can be generated automatically (e.g., Pulla *et al.*, 2001;
282 Richardson *et al.*, 2014; Magnani, 2014; Barone *et al.*, 2018; Bullenkamp *et al.*, 2022).

283
284 Beyond their role as simple visualization tools, 3D models provide crucial data,
285 particularly metric data that cannot be directly obtained from 2D images. These
286 advancements have revitalized morphometric studies of lithic artifacts, offering
287 methodological advantages, especially in terms of reproducibility and precision compared
288 to traditional manual measurements using calipers (e.g., Lycett *et al.*, 2010; Lamotte &
289 Masson, 2016; Herzlinger *et al.*, 2017; Herzlinger & Grosman, 2018; Aprao *et al.*, 2019;
290 Garcia-Medrano *et al.*, 2020; Bustos-Pérez *et al.*, 2024; Di Maida, 2023; Smith *et al.*, 2024).
291 These developments minimize inter-observer biases and eliminate optical distortions and
292 aberrations common in purely 2D-based analyses. Measurements derived from 3D models
293 include linear, angular, and volumetric dimensions, enabling more comprehensive analyses
294 of lithic artifacts, including convexity, concavity, symmetry, and asymmetry.

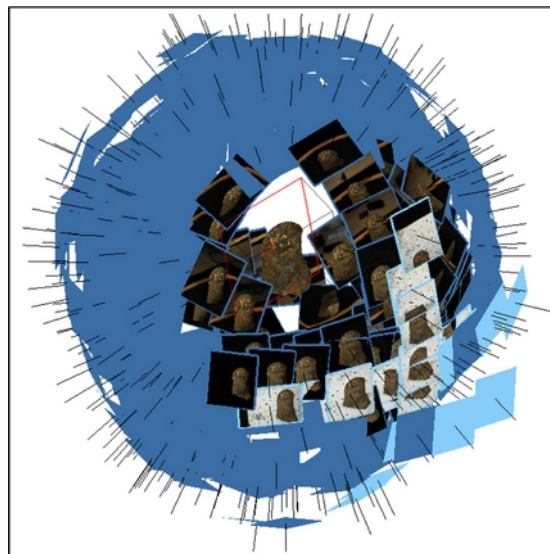
295
296 Among the various 3D digitization methods currently available, here we focus
297 exclusively on photogrammetry. This approach currently offers the best balance between
298 budget constraints and image quality (resolution, accuracy, and texture extracted directly
299 from the images used for 3D reconstruction; Mathys *et al.*, 2013; Porter, 2016; Medina,
300 2020). **This method is accessible for under €2,000, unlike 3D laser scanners or structured**
301 **light scanners (not to mention CT scans, which allow internal analysis of objects — a**
302 **feature with limited relevance for lithic artifacts). These devices can become very expensive**
303 **while providing results comparable to those obtained through photogrammetry.** Moreover,
304 open-source software solutions, such as Colmap® (Schönberger, 2016) and Meshroom®
305 (Griwodz, 2021), facilitate the post-processing steps required for photogrammetric
306 digitization.

307
308 Widely documented in the literature, particularly in Luhmann's reference book on close-
309 range photogrammetry (Luhmann, 2019), this reconstruction technique has evolved over
310 the last 180 years. With the advent of digital technologies in the late 2000s and the
311 implementation of SIFT-type algorithms (Lowe, 2004), these techniques have been
312 modernized and are now highly effective. They enable the automated execution of a well-
313 established processing workflow: image phototriangulation, depth map generation, and
314 textured triangular mesh generation.

315
316 Here, the photogrammetric method was implemented using a Nikon D850 DSLR
317 camera combined with a fixed focal length 60mm Nikon macro lens and a GODOX AR400
318 ring flash. Two linearly polarized filters, positioned perpendicularly to each other on the
319 flash and the lens, significantly reduced specular reflections often produced by siliceous
320 materials. Additionally, a colorimetric calibration target (ColorChecker®) and a geometric
321 calibration target (a machined aluminum plate with markers precisely positioned to within a
322 few hundredths of a millimeter) were included as part of the image series.

323
324 Furthermore, to best adapt the shooting geometry to the shape of the objects, no
325 turntable or automated system was used. Instead, images were manually positioned to
326 ensure complete coverage of the object's surface while maintaining a nearly constant
327 distance from the digitized surface. **In order to get the best resolution of the native images**

328 (and thus the resulting 3D model), the distance to the object is fixed by the minimal focus
329 distance enabled by the macro lens (in our case with the Nikon 60mm macro we have
330 roughly 32 cm). This method was applied to a Mousterian scraper from the cave site of
331 Pech-de-l'Azé I (Dordogne, France; Fig. 6). In this configuration, the native image
332 resolution of the object is approximately 0.01 mm, and the expected reconstruction
333 resolution is better than 0.05 mm. The accuracy of scaling is roughly the same order of
334 magnitude as the native resolution on the object. Depending on the object complexity,
335 between 200 and 500 images are required to get a complete coverage with the highest
336 resolution possible with the macro lens 60mm. The amount of pictures could be reduced,
337 fixing a higher distance to the object, but the level of details of the 3D model finally obtained
338 will be depreciated.



339
340
341
342
343
344
345
346
347
348

349 **Figure 6** - Example of acquisition geometry for a lithic artifact, generated
350 using Metashape software. Scraper from Pech-de-l'Azé I (Dordogne,
351 France). The poses (positions and orientations) of the pictures relative to the
352 object are presented by the blue rectangles (dark blue rectangles present
353 the poses of the images used for the 3D reconstruction and the light blue
354 ones the poses of the images used for the scale calibration). However, the
355 black axis is a redundant way to also show the poses of the pictures.

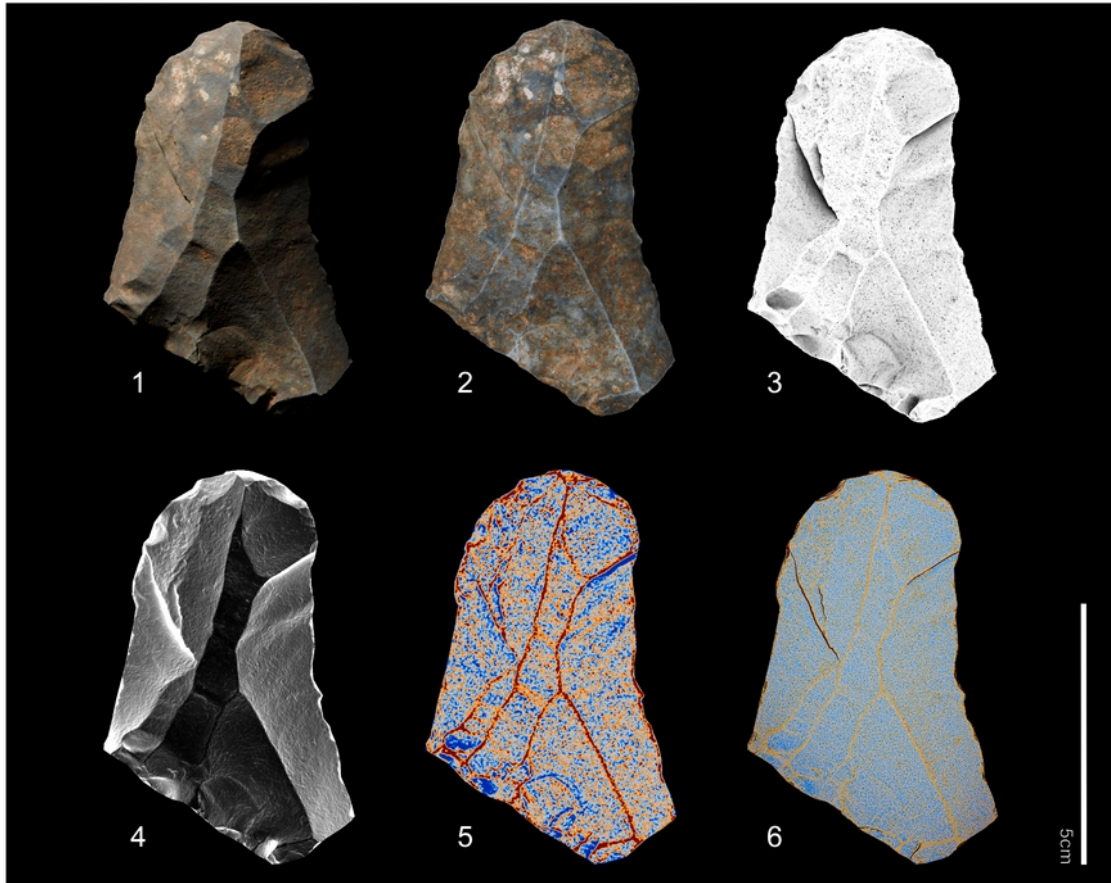
356 The second part of the processing focuses on rendering methods that generate 2D
357 representations from the produced 3D model. Multiple approaches can be considered,
358 which can be categorized into two main types (Fig. 7):

359
360
361
362
363
364
365
366
367
368
369
370

- *Using a 3D visualization tool (e.g., Meshlab) or a 3D rendering engine (e.g., Blender).* This option relies on rendering solutions from the fields of visualization and 3D animation. One example is the use of the open-source software Blender to set up the desired scene (choosing the material type for realistic or artificial BRDF adjustments, selecting the type and orientation of lighting). This approach offers limitless possibilities. Figure 7 presents two examples (Fig. 7, no. 1 & 2) that can be produced using Blender.
- *Using a 2.5D raster or depth map.* A 2.5D digital elevation model is extracted from the 3D model from a chosen viewpoint (either orthometric or central projection). Various tools commonly used in Geographic Information Systems (GIS) can be utilized to generate different types of shaded models. Figure 7 presents several types and

371
372
373
374
375
376

parameter settings (non-exhaustive) for shading the scraper. View No. 3 shows the rendering using ambient occlusion (Tarini *et al.*, 2006) while views No. 5 and 6 illustrate derivatives of the 2.5D raster, specifically the calculation of indices characterizing local convexity or maximum local curvature (computed using SAGA GIS software following Conrad *et al.*, 2015).



378
379
380
381
382
383
384
385

Figure 7 - Representations derived from the 3D model (photogrammetry). 1) Textured rendering with directional lighting produced using Blender. 2) Textured rendering with diffuse lighting produced using Blender. 3) Shaded rendering with ambient occlusion, directly extracted in 3D from Agisoft Metashape. 4) Shaded rendering based on the Skyview Factor, generated using SAGA GIS. 5) Convexity index map, generated using SAGA GIS. 6) Maximum curvature map, generated using SAGA GIS.

386
387
388
389
390
391
392
393
394

Far more than simple visual representation systems, various 3D acquisition methods enable in-depth morphometric analyses. They also provide a contact-free means of handling, presenting, and sharing rare and fragile artifacts. However, to achieve accurate results, these methods require lengthy and complex data processing, demanding advanced expertise in 3D modeling as well as high (and costly) computational power. In most current publications, 3D digitization is not justified, and the perception of lithic industries remains confined to traditional representation systems (drawings, photographs), supplemented by counts, targeted measurements, and statistical treatments of the data.

3.4. Reflectance Transformation Imaging (RTI) of lithic artifacts

396 Reflectance Transformation Imaging (RTI) combines the advantages of both drawing
397 and photography. Based on the Polynomial Texture Mapping (PTM) approach, RTI was
398 developed by a research team at Hewlett-Packard led by Tom Malzbender (Malzbender *et*
399 *al.*, 2001) and was quickly applied to the fields of natural sciences and cultural heritage
400 (Mudge *et al.*, 2008; Earl *et al.*, 2010a, 2010b, 2011; Cultural Heritage Imaging, 2018). RTI
401 relies on two key algorithms: Polynomial Texture Mapping (PTM) and Hemispherical
402 Harmonics (HSH). We will use the HSH in this work. The main difference between PTM
403 (the original algorithm) and HSH (the more recent algorithm) is that the latter offers
404 enhanced capabilities for handling high-frequency surface details by approximating the
405 reflectance behavior across the surface using spherical harmonics. This method is
406 particularly useful for capturing fine textures and subtle variations (Robitaille, 2025).

407

408 This method, which requires minimal time, is also low-cost, requires non-specialized
409 equipment, and allows for the visualization of an object's interactions with artificial lighting.
410 By utilizing the object's reflectance properties and adjusting the angle of light incidence, it
411 becomes possible to enhance the perception of its microtopography (Masson Mourey,
412 2019).

413

414 RTI enhances our ability to observe and analyze details, providing a means of bringing
415 to light what is often difficult to see with the naked eye, such as use-wear traces, surface
416 irregularities and alterations, or polishes. It has been applied to a wide range of objects of
417 different sizes (Cosentino, 2013 ; refer to the detailed guide on RTI applied to
418 macrophotography), shapes, and environmental contexts, including numismatics,
419 epigraphy (e.g. Chapman *et al.*, 2017), architecture, and painting (Mudge *et al.*, 2006 ;
420 Kotoula & Earl, 2015). While this method has long attracted interest for the study of rock art
421 or portable art objects (e.g., Mudge *et al.*, 2006; Lymer, 2015; Horn *et al.*, 2018; Masson
422 Mourey, 2019; Kosciuk *et al.*, 2020; Robitaille *et al.*, 2024), as well as on bone and fossil
423 surfaces (Hammer *et al.*, 2002; Newman, 2015; Purdy *et al.*, 2011; Morrone *et al.*, 2019 ;
424 Desmond *et al.*, 2021), or isolated stone tools (Pawlowicz, 2015; Fiorini, 2018), it has never
425 been used in the analysis or presentation of a lithic assemblage or lithic industry—only for
426 isolated artifacts. The RTI has recently been adapted at the microscopic scale for the
427 functional analysis of lithic artifacts, with the goal of providing detailed documentation of
428 use-wear traces, which were previously difficult to access using conventional imaging
429 methods (Robitaille, 2025).

430 3.4.1. Principle, equipment, and method

431 Principle

432 Reflectance Transformation Imaging (RTI) creates an interactive image by capturing a
433 series of photographs from a fixed position while illuminating the subject's surface from
434 different light angles. When light interacts with a surface, four main phenomena can occur:
435 absorption, transmission, diffusion, and reflection. Absorption occurs when the light flux is
436 taken in by the material. Transmission happens when the light passes through the medium
437 without being absorbed. Diffusion takes place when light is scattered in all directions within
438 the medium. Finally, reflection occurs when the incident flux is redirected into the same
439 hemisphere from which it contacted the surface (Vila, 2017, p.18). RTI is based on the
440 principle of reflection. Processing software utilizes surface normal information (the normal
441 vector at a point on a surface is perpendicular to the tangent plane at that point) to compute

442 the deviation of light rays across the surface (Cultural Heritage Imaging, 2018). To perform
443 these calculations, it is essential to know the precise position of the incident light source for
444 each captured image. The phenomenon of reflection itself can be divided into two distinct
445 sub-phenomena: specular reflection and diffuse reflection (Vila, 2017). On smooth
446 surfaces, reflection follows the law of specular reflection: the angle between the incident
447 light ray and the surface normal is equal to the angle between the normal and the reflected
448 ray. In contrast, on rough or textured surfaces, light scatters in multiple directions,
449 producing diffuse reflection.

450

451 One of RTI's main advantages is its ability to deduce the surface normal for each pixel
452 from the computed model. In a Cartesian coordinate system, this normal is defined by three
453 components: x, y, and z. By combining this information with variations in the intensity of the
454 red, green, and blue (RGB) bands depending on the direction of a light source, RTI
455 generates a normal map. The result reveals fine surface details and textures that may not
456 be visible in a static photograph. Although the output is a 2D image, it is often described as
457 "2D½" because it contains enhanced visual information that allows for a more three-
458 dimensional perception of the object.

459

460 There are several RTI capture methods, including fixed domes or motorized rotating
461 arcs (e.g., Earl *et al.*, 2011; Malzbender *et al.*, 2001; Mudge *et al.*, 2005 ; Porter *et al.*,
462 2016). Here, we present the Highlight-RTI (H-RTI) method, developed through the
463 combined efforts of Cultural Heritage Imaging (CHI), Hewlett-Packard Labs (HP Labs), and
464 the University of Minho, Portugal (Mudge *et al.*, 2006). This method determines the position
465 of the artificial light source (incident angle) by analyzing reflections on a reflective sphere
466 captured in each photograph. It then uses interpolation to calculate how light interacts with
467 the object from all directions (Cultural Heritage Imaging, 2018; Mudge *et al.*, 2006).
468 Although H-RTI may be less precise in determining light position compared to dome RTI or
469 motorized arcs, it offers the advantage of requiring no specialized equipment, is easily
470 transportable (e.g., in a backpack), and is easy to use, requiring only minimal training.

471 *Equipment*

472 The equipment required and the method used for H-RTI have been extensively detailed
473 (Cultural Heritage Imaging, 2018); here, we adapt them for lithic industries (Fig. 8). A DSLR
474 camera is mounted on a stand to maintain a stable and zenithal position relative to the lithic
475 artifact. The subject is placed on a matte black background to avoid unwanted reflections.
476 Scaling the artifact remains a challenge, as it is not possible to create an orthophotograph,
477 as can be done with photogrammetry, which may lead to distortions. To minimize this
478 issue, it is recommended to use medium focal length lenses (between 28 mm and 100 mm)
479 to prevent optical distortions caused by wide-angle or telephoto lenses (*ibid*, 2018, p.8-9).
480 The camera and lens focus are set to manual mode. For artifacts smaller than 2 cm,
481 imaging is performed using a binocular microscope (Leica S8 APO, x10) along with the
482 same camera.

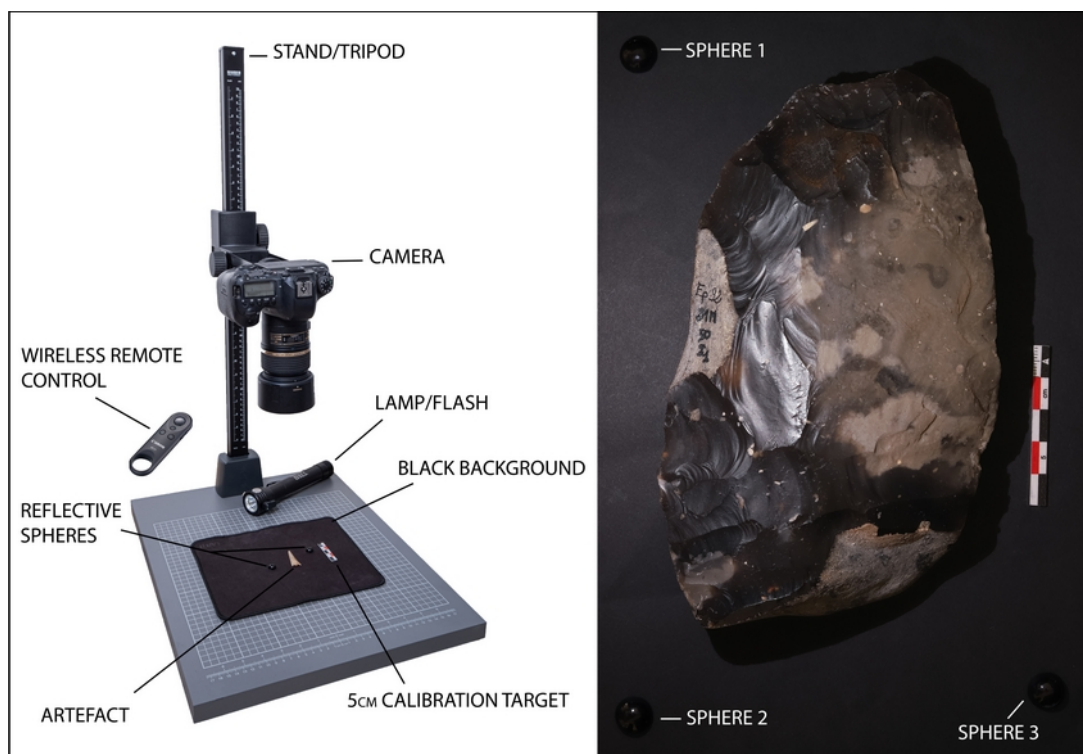
483

484 Two or three black, reflective spheres are placed near the subject. The size of these
485 reference spheres depends on the size of the artifact as well as the distance from the
486 camera sensor, and they should correspond to 250 pixels (*ibid*, 2018). The spheres should
487 be positioned at the same height as the subject's surface, ensuring they are fully within the
488 depth of field, thereby guaranteeing proper focus. It is important to ensure that they are not
489 placed too high, to avoid casting shadows on this surface, nor too low, to prevent them
490 from being constantly in the subject's shadow. If one of the spheres becomes invisible due

491 to grazing light, the use of another sphere will help identify the position of the light source.
492 The size of the spheres used ranges from approximately 1 mm to 30 mm. If photography is
493 conducted under natural light (outdoors during the day), which is not recommended, it is
494 preferable to use high-powered flashes to counteract ambient light. A neutral density
495 (polarizing) filter can also be used if necessary.
496

497 Photographs should be taken without touching the camera to avoid any vibrations or
498 movements that could introduce calculation errors. The shutter should be triggered
499 remotely, using either a wired or wireless remote control, the camera's Bluetooth
500 smartphone app, or a computer. Make sure that the object remains perfectly still, even at
501 the micron scale, in order to avoid any errors in the calculations and the generation of a
502 blurry model. For RTI acquisition of artifact profiles and striking platforms, the artifact can
503 be stabilized using adhesive putty or placed in a tray of sand. A 5 cm scale marker is
504 positioned near the subject.
505

506 A ColorChecker® color chart can also be used to properly calibrate white balance
507 during post-processing. If the subject is difficult to access—which is rarely the case for a
508 lithic artifact—it is recommended to perform an initial data processing step to ensure the
509 RTI quality is sufficient and that no issues are present.
510



512 **Figure 8** - Left: installation and equipment required for RTI acquisition.
513 Right: One of the fifty raw photographs from an RTI image sequence (3
514 visible spheres) - Biface from Cagny l'Épinette (Somme, France).

515

517 **Camera settings:** Each photograph in the series must have identical settings.
518 Therefore, the camera is set to manual mode. Images should be captured in JPEG format
519 (or RAW+JPEG). The ISO value should be kept between 100 and 400 (low ISO). The
520 aperture setting depends on the morphology of the object but generally ranges between
521 f/5.6 (for very flat objects) and f/13 to maximize the sharpness of the photograph. In some
522 cases, for example, side views of an artifact or an irregular core, a smaller aperture (higher
523 f-stop) is necessary to extend the depth of field. The exposure time varies based on the
524 ISO and aperture settings, and the image should be slightly underexposed to prevent
525 overexposure. For these settings, it is important to take into account the raw material and
526 the surface condition of the lithic artifact. A polished or worn surface is more likely to create
527 overexposed areas. Since settings must remain consistent from the first to the last image,
528 this factor must be accounted for before starting the acquisition process. Additionally, the
529 "Auto Image Rotation" function is disabled, and white balance is set manually. The lens
530 focus is also adjusted manually (you can use the camera's digital zoom to fine-tune the
531 focus with precision)

532

533 **Image acquisition method:** All photographs are taken in complete darkness (or with a
534 very slight diffuse light), ensuring that neither the subject nor the camera is moved. In order
535 to create a virtual dome above the subject, photographs are taken at different lighting
536 angles: 5° - 15° - 40° - 65°, while rotating around the object in 12 equal steps (30° between
537 each step, similar to the positions on a clock). Additionally, a single photograph is taken
538 with a lighting angle close to 90°. This image, not included in the RTI process, provides a
539 simple lighting setup that will facilitate the automatic selection of the subject during post-
540 processing (in Photoshop). Indeed, it is not possible to make this selection automatically
541 with the RTI images in normal mode, nor with the photographs taken with grazing light. The
542 light source remains at a constant distance from the subject throughout the process, ideally
543 four times the subject's diameter (or between two and four times its diameter, as
544 recommended by Cultural Heritage Imaging, 2010). The reflective sphere should be placed
545 next to the subject, but not too close to avoid casting shadows that could distort
546 calculations (Vila, 2017). To mitigate potential errors caused by grazing light, it is advisable
547 to use two spheres placed on opposite sides of the subject. If one sphere is obscured by
548 the object's shadow, the other will remain well-lit. The same method is applicable for RTI
549 acquisitions using a binocular microscope (Hughes-Hallett *et al.*, 2021; Goldman *et al.*,
550 2018). A documentation sheet is created for each RTI session, recording the author's
551 name, date and location, number of photographs and corresponding file numbers,
552 equipment used, and any issues encountered.

553

554 **Data Processing: RTI Processing with Relight® - Quick Guide**

555

556 The RTI file is generated using the Relight® software (version 2023.02; Ponchio *et al.*,
557 2019). A detailed description of the processing workflow is available at the following link:
558 [https://github.com/ExeterDigitalHumanities/rti/blob/main/RTI%20processing%20with](https://github.com/ExeterDigitalHumanities/rti/blob/main/RTI%20processing%20with%20RelightLab%20v2.pdf)
559 [%20RelightLab%20v2.pdf](https://github.com/ExeterDigitalHumanities/rti/blob/main/RTI%20processing%20with%20RelightLab%20v2.pdf). Below is a summary of the main steps involved in the process:

560

- 561 - Go to the "File" menu and select the "New" tool to import the photos into the software.
- 562 - Use the "New Sphere" tool to indicate the position of the reflective sphere, then you
563 select three points on the periphery of your sphere to form a circle.
- 564 - In the "Edit" menu, use the "Find Highlights" tool. The software automatically detects
565 light reflected in the sphere and calculates the lighting angle.

- 566 - Check the light position on each photo. Adjust if necessary by dragging the green or
567 red point (if no reflection was detected in the image) with a long mouse click.
568 - Go to the "Export" menu and choose the "Export RTI" tool.
569 - In the "Basis" tab, select "HSH 27 - Hemispherical harmonics."
570 - Choose the "RTI" format and click "Build" to finalize the process.

571

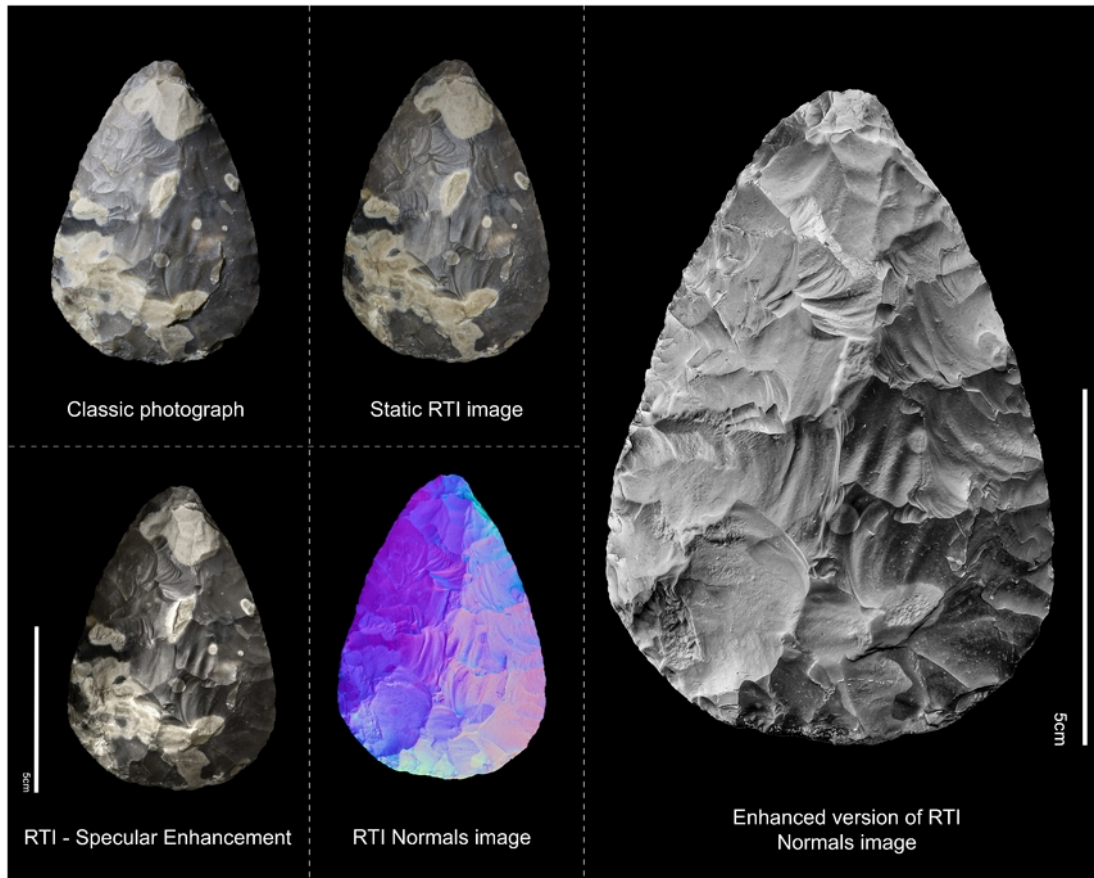
572 **RTI Visualization with RTIViewer®** : The RTI file is opened in a visualization software,
573 RTIViewer® (version 1.1; Cultural Heritage Imaging, 2013). In this software, photographs
574 taken from different lighting angles can be viewed in various modes. The first mode, "Static
575 RTI image", removes specular reflections and highlights, allowing interactive changes in
576 the lighting direction. This mode accurately conveys color and patina details of lithic pieces.
577 The second mode, "Specular Enhancement", is similar to the first but reduces color
578 information while enhancing reflectance values. The third mode, "Normals mode", derives
579 the unit normal vector for each pixel based on the reflectance model. This visualization
580 mode represents the x, y, and z components using false colors: red, green, and blue,
581 respectively, in a 2D image. From the RTIViewer® interface, a JPEG file can be created
582 using the "Snapshot" tool, which is readable in any image processing application. **From this**
583 **software, you will also have the ability to create bookmarks, pre-define close-up views, a**
584 **specific lighting angle, or frame a particular area, which is a useful tool for sharing with**
585 **colleagues.**

586

587 **Post-Processing in Photoshop®**. In Photoshop® (or **Photopea for a free software**
588 **available online : <https://www.photopea.com>**), the lithic artifact is automatically cropped and
589 then manually refined before being placed on a uniform black or white background. To
590 enhance visual aesthetics, the RTI Normal mode is converted to black and white using
591 Photoshop®. This transformation is performed via "Adjustments" → "Black & White",
592 allowing for individual adjustments to each color channel (red, yellow, green, cyan, blue,
593 and magenta). Some minor edits and corrections (e.g., texture, clarity, and sharpness
594 adjustments in Camera Raw) may be applied. However, it is crucial to note that this stage
595 results in a loss of methodological reproducibility. Therefore, all modifications are limited to
596 global adjustments, avoiding targeted alterations to specific artifact areas. To preserve
597 color information, a Static RTI or a standard photograph is always placed next to the black-
598 and-white Normal mode.

599

600 To accurately document an artifact, it must be represented from several predefined
601 angles, including the main view, profile views, butt view, and sometimes the reverse side
602 view. These views are aligned with the reference image, with object rotations set at 90°
603 increments. The "American method" is used, displaying the profile view from the object's
604 side (e.g., Der Arahamian & Abbès, 2015). Intermediate 45° rotations may also be used to
605 highlight retouching, with the angle value indicated. Although technological analysis can
606 often be performed more effectively using RTI results than with the naked eye, additional
607 graphic elements (such as arrows) may be added to facilitate diacritical reading. In such
608 cases, standard lithic drawing conventions (Dauvois, 1976, p. 129) are followed. These
609 annotations are the only interpretive elements introduced and remain easily distinguishable
610 from the RTI-generated data (Fig. 9).



613
614
615
616
617

Figure 9 - Different RTI visualization modes and comparison with standard photography. Experimental handaxe - captured using a Canon 6D Mark II DSLR with a Canon 50mm f/1.8 lens - settings: f/14, 1/10 sec, ISO 100.

618 Supplementary data are provided to facilitate the testing of the proposed method. These
619 data concern two handaxes: the first is an experimental handaxe shown in Figure 9; the
620 other is an Acheulean handaxe, discovered at the Cagny l'Épinette site (Somme, France),
621 and shown in close-up in Figure 10. For the first, you have the raw results from ReLight and
622 RTIViewer. For the second, you have these same files but also unmodified photographs
623 allowing you to do the manipulation yourself.
624

625 3.4.2. Results

626 Production time and storage

627
628 The estimated average time required to create an RTI view of a lithic artifact is as
629 follows:

- 630 - Setup phase: approximately 5 minutes. Once completed, this step does not need to
- 631 be repeated for subsequent views.
- 632 - Photographic acquisition: also around 5 minutes.

- 633 - RTI file creation in Relight® and JPEG export from RTIViewer®: less than 5
634 minutes, though this step is highly dependent on computer performance.
635 - Photoshop® processing and plate creation: between 5 and 10 minutes. (This step
636 is common to all methods discussed in this study, whether photography or drawing,
637 as they all require post-processing and digital graphic work.)
638

639 The total time required to generate an RTI view is around 20 minutes, meaning that for
640 three views, the complete processing of an artifact takes approximately one hour. Naturally,
641 this process takes longer when producing the first RTIs, but with experience, the workflow
642 becomes more efficient.
643

644 Each view is made up of approximately 50 to 100 photos, each taking up about 5
645 megabytes of storage, totaling 250 megabytes per view. The RTI file itself is around 700
646 megabytes (but this size can easily be reduced by cropping the model before export),
647 resulting in 1 gigabyte of data per view. While this may appear heavy, however it is
648 important to note that storing the RTI files is unnecessary if the original photos are
649 preserved, significantly reducing storage requirements..
650

651 **Visualization of knapping marks**

652

653 By its very principle, RTI reveals surface reliefs and micro-reliefs with greater precision
654 than traditional photography, including knapping scars, such as ripples, hackles, negatives
655 of micro-flakes resulting from fine retouching or use, and an easy distinction between
656 concavities and convexities (Fig. 10). The final image quality depends solely on the
657 specifications of the camera and lens used. This allows for macro views capturing fine
658 details on edges, as well as producing images of very small objects, such as bladelets (Fig.
659 11). Most importantly, multi-directional lighting makes it easy to identify knapping scars
660 regardless of their location on the artifact, rather than being limited to the raised areas
661 highlighted by conventional digital photography lighting. While some knapping scars can be
662 discerned through direct examination in natural light, RTI images can confirm observations
663 and reveal previously unnoticed details. Additionally, it is difficult—if not impossible—to
664 capture all the key details of an artifact in a single photograph, whereas RTI Normals mode
665 achieves this comprehensively.
666

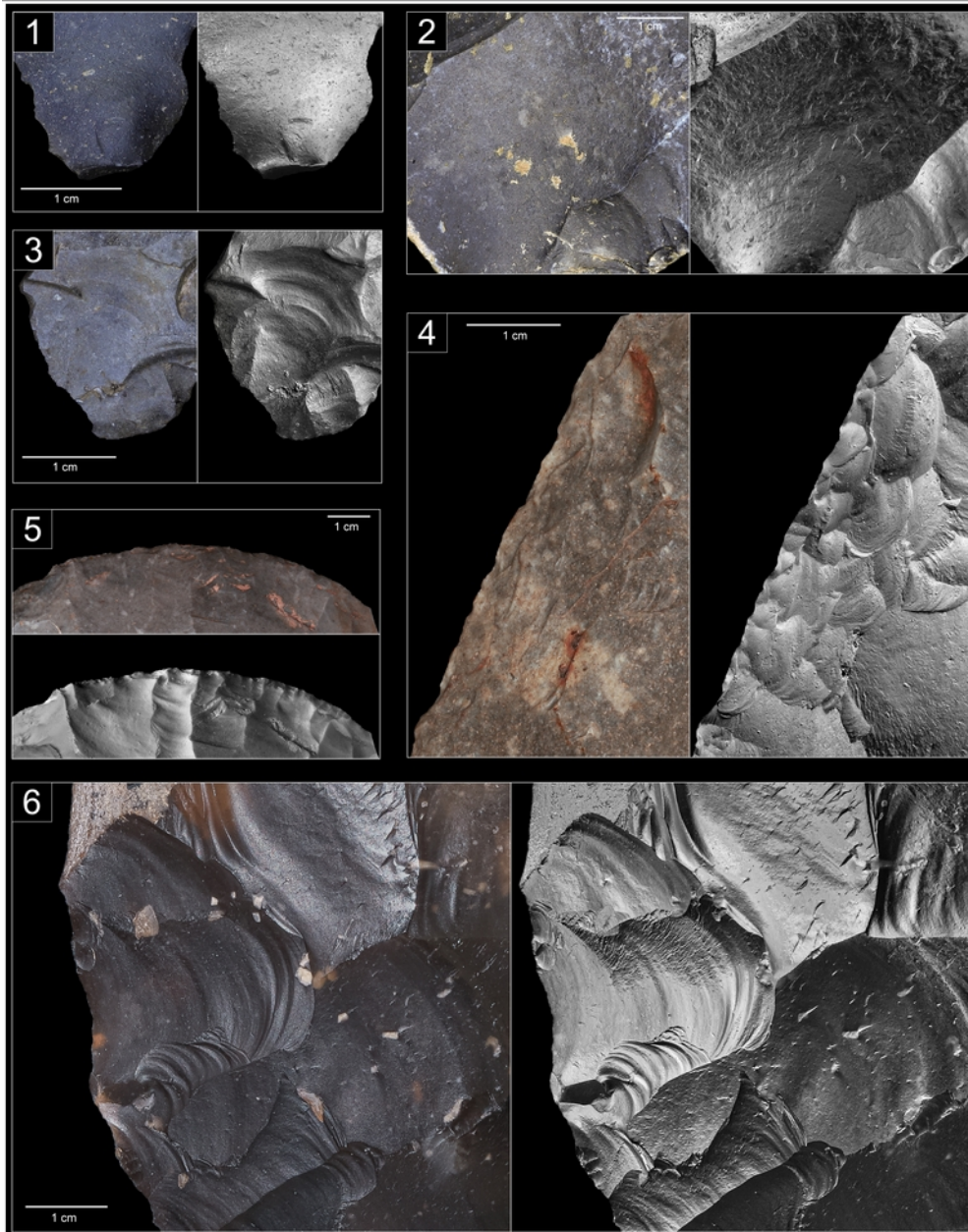
667 **Visualization of artifacts based on material and patina**

668

669 While RTI Normals mode enhances the grain of the material, it removes color, which
670 can make it harder to immediately recognize a specific raw material. However, this
671 limitation is relative, as attempting to identify raw materials from a single overview image is
672 already difficult.
673

674
675
676
677
678
679
680

681
682
683
684
685
686
687
688
689
690
691
692
693
694
695
696
697
698
699
700
701
702
703
704
705
706
707
708
709
710
711
712
713
714
715
716



717
718
719
720
721
722
723
724
725
726
727
728
729
730
731

Figure 10 - Comparison of the representation of knapping marks between a standard photograph with diffuse lighting and an optimized version using the normal map from RTI. **1)** Detail of the proximal part of a blade (Grotte XVI, Dordogne, France). The bulb and its bulb scars, as well as the fine lip, are clearly visible. **2)** Detail of a removal on a Quina scraper (Grotte XVI, Dordogne, France). The hackles resulting from the hackle of the material stand out with great precision near the ridges, allowing the chronology of the removals to be determined. **3)** Close-up view of a removal on a flake (Grotte XVI, Dordogne, France). Beyond the hackles, the ripples from the propagation of the shockwave are distinctly visible. **4 & 5)** Detail of the edges of two handaxes (Durcet-Saint-Opportune, Normandy, France). RTI highlights the micro-removals linked to retouches on the edge of the tool. **6)** Close-up view of an edge and multiple removals on a handaxe (Cagny-L'Épinette, Somme, France), illustrating all the mentioned features: ridges, hackles, negative bulb, ripples, cortex, retouch, etc

732 In some cases, RTI can even overcome challenges faced by conventional
733 photography. Certain types of alterations can make an artifact difficult to analyze visually,
734 especially when vermiculations create sinuous veins and patterns on the surface. For
735 example, on a heavily patinated (vermiculated) transverse scraper, a conventional
736 photograph may fail to distinguish technological details, which could be confused with the
737 vermiculated patina. In contrast, RTI Normals mode eliminates color variations from the
738 surface and patina, providing a homogeneous representation of reliefs and micro-reliefs
739 present on the piece (Fig. 12, no.1).

740

741 Translucent materials are generally challenging to capture using photography or
742 scanning. Light passes through the piece, reflecting very little, which prevents surface
743 reliefs from being clearly visible. Our results with relatively translucent chalcedony artifacts
744 show that RTI effectively corrects this issue (Fig. 12, no.2). Similarly, highly patinated flints,
745 which appear completely white due to surface alteration (Caux *et al.*, 2018), are difficult to
746 photograph because they quickly lead to overexposure. RTI removes these reflections,
747 producing an image with even lighting across the entire artifact (Fig. 12, no.3).

748

749 The extremely high precision provided by RTI imaging allows the reader to visually
750 assess the surface condition of artifacts. For example, RTI reveals that the ridges of a
751 minimally altered piece exhibit fine linearity. In contrast, on pieces altered by friction, the
752 ridges appear less well-defined and more diffuse. Furthermore, RTI eliminates reflections
753 and highlights created by highly lustrous surfaces, making it possible to distinguish
754 between lustre and blunting.

755

756

757 **RTI vs. Photogrammetry**

758

759 To objectively assess the differences in rendering between the two methods, a pixel-by-
760 pixel comparison was performed between the normal maps obtained using RTI and
761 photogrammetry. First, the RTI reference image was aligned via phototriangulation within
762 the photogrammetric dataset. This step ensures that the normal map generated from the
763 photogrammetric model has a central projection that is strictly comparable to that of the RTI
764 reference image. Then, the angle formed by the two normal vectors for each pixel was
765 calculated using the dot product, producing a map of angular differences (Fig. 13).

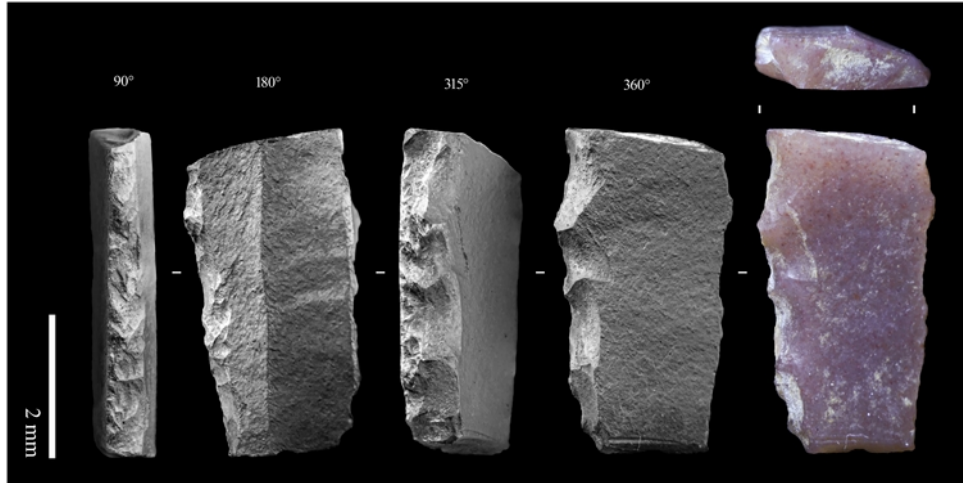
766

767 From a practical and technical perspective, the normal map generated from the 3D
768 model provides a satisfactory global visualization, where each removal of material can be
769 isolated and identified. However, technological analysis is limited due to the lack of surface
770 detail. In contrast, RTI-generated normal maps offer a more detailed restitution, capturing
771 not only the removals but also the marks left by the detachment of material (hackles), as
772 well as undulations and subtle hinge fractures. This allows the reader to reconstruct the
773 chronology of removals without requiring physical manipulation of the artifact. This contrast
774 is clearly visible in the angular difference map (Fig. 13). The average angular difference
775 between the normal vectors is approximately 10 to 20° on flat surfaces, reaching up to 50°
776 along ridges and micro-reliefs. It is precisely the recognition of these micro-reliefs that is
777 crucial for a comprehensive understanding of an artifact

778

779

780

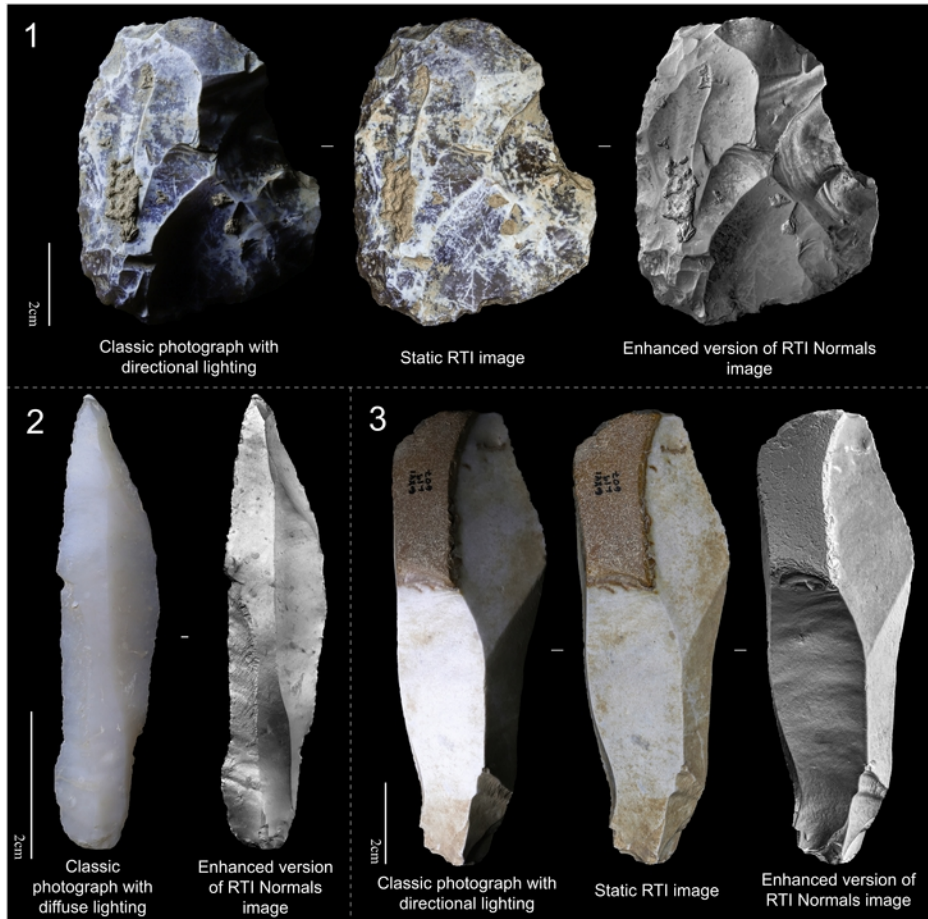


782 **Figure 11** - Macro-RTI visualization of a small lithic artifact: Retouched
 783 bladelet, Upper Paleolithic, Grotte XVI (Dordogne, France). Binocular
 784 magnifier Leica S8 APO - x10 - Reflex camera Canon 6D Mark II - 1/20
 785 seconds - 100 ISO.

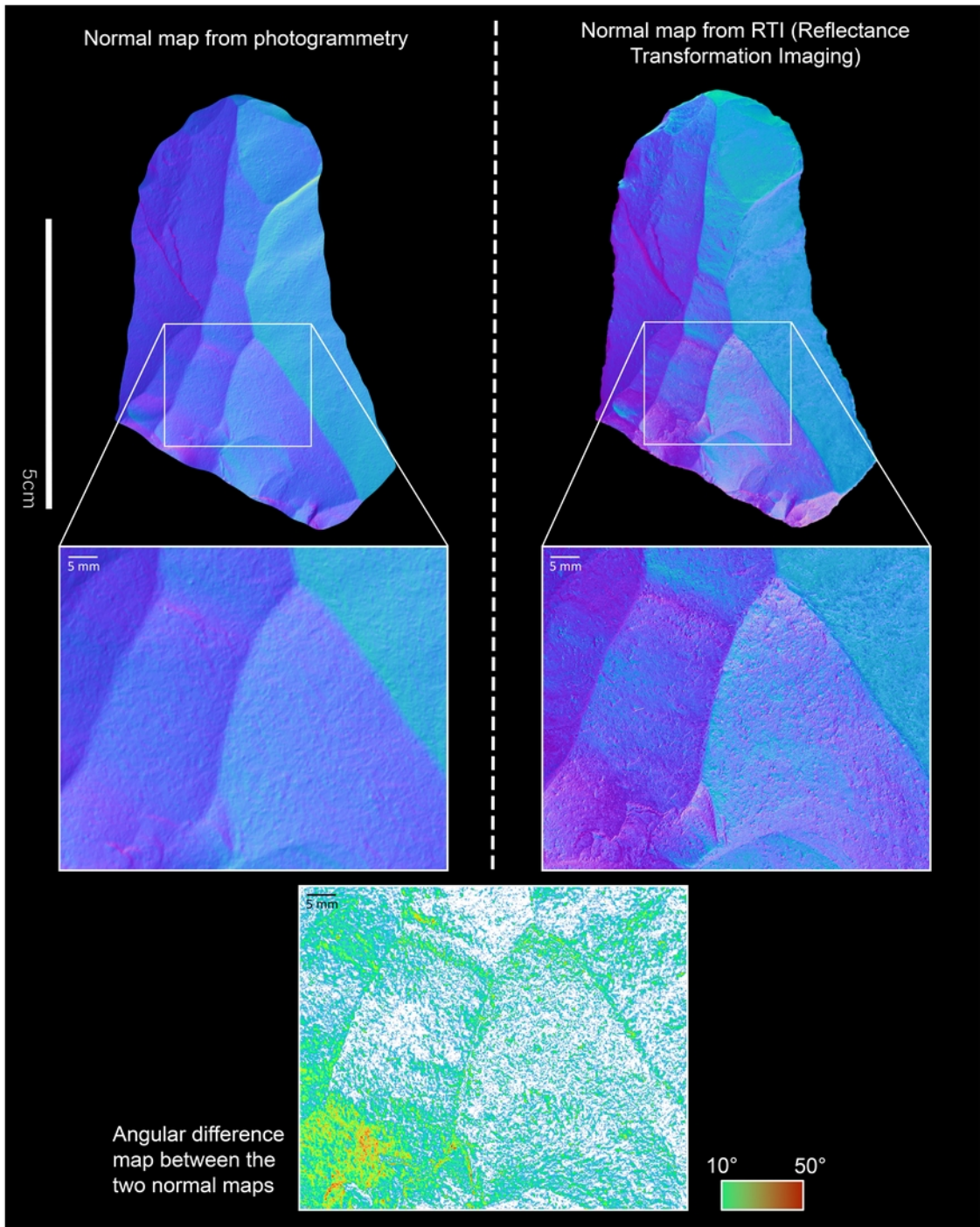
786

787

788



789 **Figure 12** – Visualization of different raw materials and patinas on three
 790 pieces from Grotte XVI (Dordogne, France). **1.** Scraper with vermiculated
 791 patina (Middle Paleolithic). **2.** Blade in translucent chalcedony (Upper
 792 Paleolithic). **3.** End-scraper on a blade with white patina (Upper Paleolithic).
 793 Settings : Reflex camera Canon 6D Mark II – Lens Canon 50mm f/1.8 – f/10
 794 – 1/20 seconds – 100 ISO.



796
797

Figure 13 - Comparison of normal maps created by photogrammetry and RTI.

798

4. Discussion and conclusion

800 Evaluating the application of different methods for representing lithic industries—such
801 as drawing, photography, 3D modeling (photogrammetry or other methods), and RTI—
802 relies on several key criteria. These include cost, time required, ease of implementation,
803 and quality of the final result (Tab. 1). However, quantifying and objectively assessing these
804 criteria is challenging due to the numerous dependent variables.

805
806 Artifact drawings stand out due to their extremely low cost in terms of materials
807 required. In contrast, techniques such as 3D scanning/microtomography require substantial
808 investment, ranging from several tens of thousands to several hundred thousand euros,
809 limiting their purchase to companies or laboratories. Photographic methods, namely RTI
810 and photogrammetry, offer a more economical alternative as they require only a good-
811 quality setup to produce publishable results. **An equipment costing between €1500 and**
812 **€2000 could be more than sufficient, as for us, a camera body costing around €1000, an**
813 **appropriate lens (e.g., macro) at €500, along with a flash and various accessories (cables,**
814 **etc.) at around €100-200, make up a functional setup. We must not forget the cost the**
815 **software either, whether it is for 3D creation software or image processing software such as**
816 **Photoshop/Illustrator.**

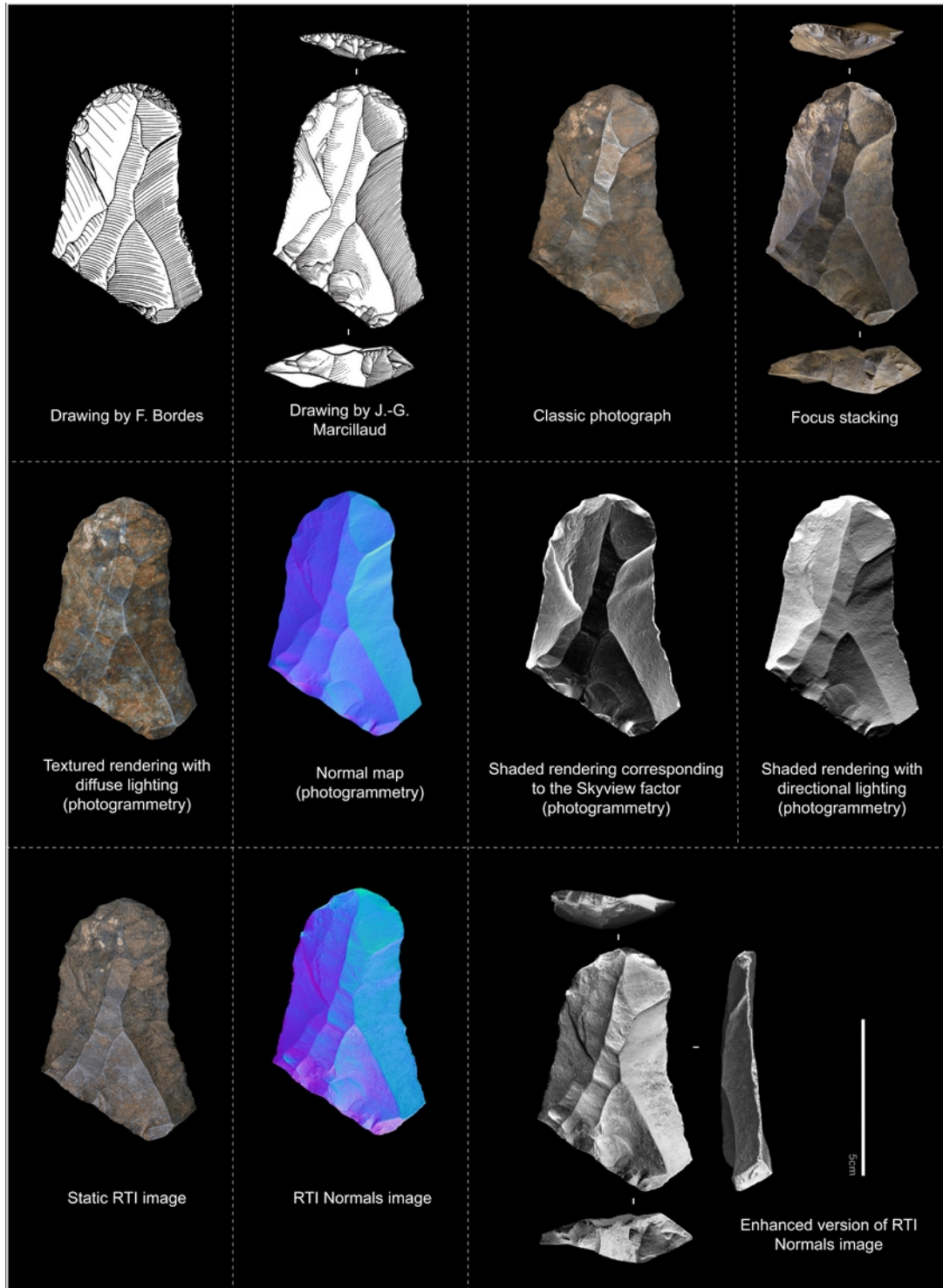
817
818 Time constraints and ease of implementation are also crucial factors, especially when
819 dealing with multiple artifacts or an entire lithic assemblage. Traditional drawings, while
820 widely used, require significant training, even for experienced illustrators, to master the
821 precise conventions needed for accuracy. Moreover, the time required for drawing varies
822 significantly depending on expertise and the complexity of the object. On average,
823 producing and digitally processing a single lithic drawing takes over an hour. Standard
824 photography is much more accessible, requires minimal training, and enables the rapid
825 acquisition of images (approximately 5 minutes per object), though post-processing can be
826 time-consuming (ranging from 5 to 15 minutes).

827
828 Photogrammetry can generate accurate 3D models using more accessible and portable
829 equipment compared to 3D scanners. Like Reflectance Transformation Imaging (RTI), it
830 requires between 30 minutes and 1 hour for a complete artifact acquisition. However, while
831 RTI processing is relatively fast (around 5 minutes), photogrammetry, despite being largely
832 automated, requires significantly more time—typically 2 to 3 hours per model. This
833 extended processing time limits its scalability when modeling a large number of objects.
834 The RTI methodology outlined in this study should be sufficient to successfully create a
835 high-quality RTI visualization.

836
837 Each method for illustrating lithic artifacts has its own advantages and limitations.
838 Drawings, while traditional and cost-effective, are subject to interpretation and can vary in
839 quality depending on the illustrator's skill. Photography, while fast and accessible, can
840 produce incomplete or interpretative results that can hinder technological analysis.
841 Moreover, photography does not provide quantitative information about the object's
842 topography. 3D scanning offers highly accurate modeling but is constrained by high
843 equipment costs, limited mobility, and expensive maintenance. Additionally, 3D scans
844 generate very large files (ranging from 5 to 30 GB), posing questions of storage and
845 transferability. Photogrammetry provides detailed 3D modeling at a lower cost than
846 scanning but lacks the precision needed for analyzing fine details, making technological
847 interpretations more challenging.

848 RTI, despite producing relatively large files (which can be easily compressed), appears
849 to be the most effective method for representing individual artifacts. It offers a balanced
850 combination of moderate acquisition time, affordable and portable equipment, and highly
851 detailed visualizations of microrelief, significantly enhancing technological analysis (see
852 Figures 14 and 15). Ultimately, the choice between these methods depends on the specific
853 needs of a given project.

854
855 In many cases where 3D modeling of artifacts is not necessary for research objectives,
856 RTI far surpasses traditional representation approaches (such as drawings and
857 photography) while remaining relatively simple to implement. Here, we have provided the
858 necessary information to make this method accessible to everyone. By ensuring that
859 discussions of lithic industries are based on a large number of illustrated items,
860 interpretations can be critically evaluated more easily based on robust visual
861 representations of artifacts.



863
864
865
866
867
868

Figure 14 - Comparison of different illustration methods for the same lithic artifact – Scraper from Pech-de-l’Azé I (Paleolithic, Dordogne, France). Photography and focus stacking exif: Nikon D850 - Sigma ART 50mm f/1.4 DG HSM - f/13, 1/8s, ISO 80 ; 3D exif: Nikon D850 - Macro 60mm - f/14, 1/320s, ISO 100 ; RTI exif: Nikon D850 - Sigma ART 50mm f/1.4 DG HSM - f/11, 0.8s, ISO 80.

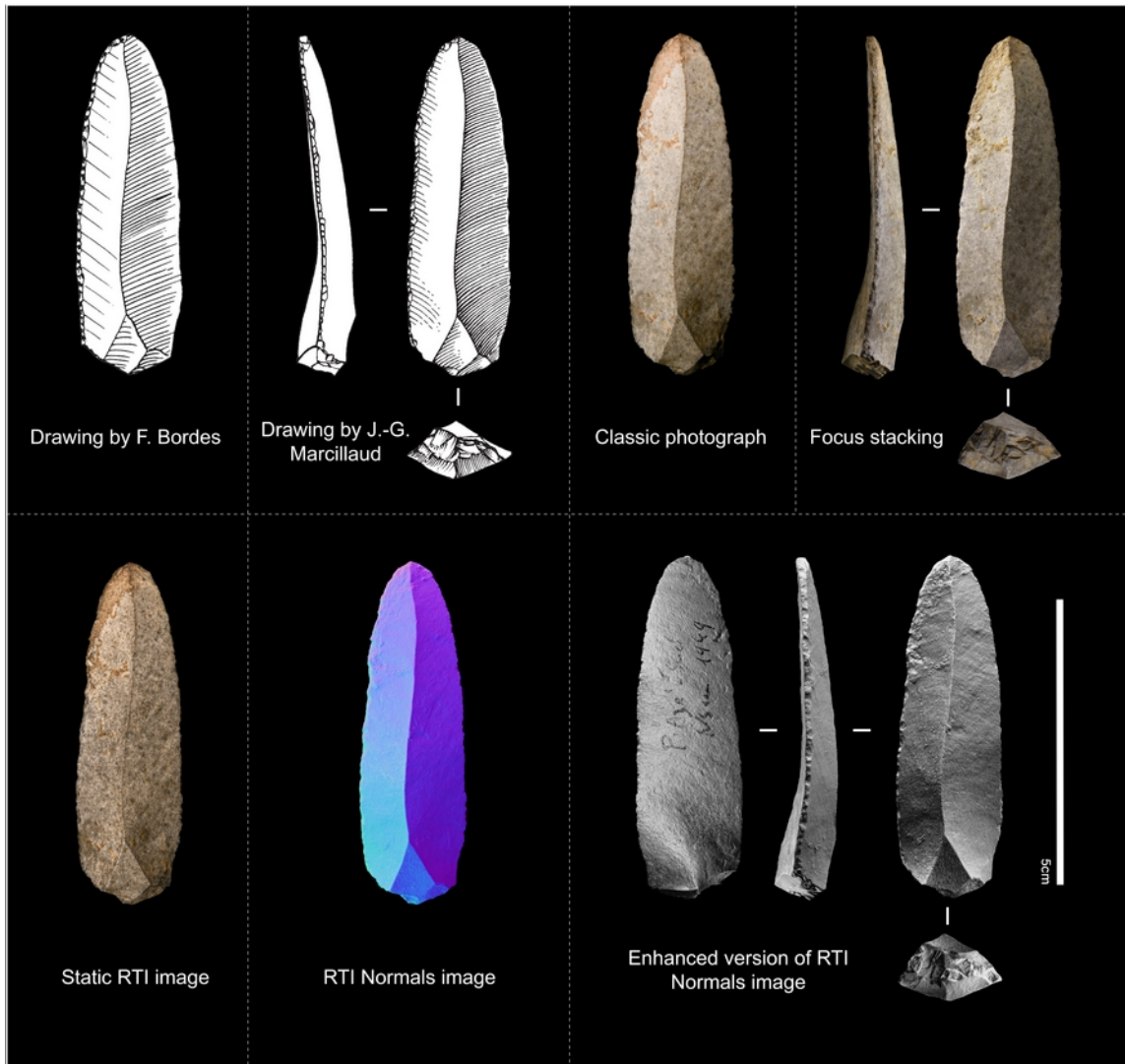


Figure 15 - Comparison of different illustration methods for the same lithic artifact – Elongated flake from Pech-de-l’Azé I (Paleolithic, Dordogne, France). Photography and focus stacking exif: Nikon D850 - Sigma ART 50mm f/1.4 DG HSM - f/13, 1/8s, ISO 80 ; 3D exif: Nikon D850 - Macro 60mm - f/14, 1/320s, ISO 100 ; RTI exif: Nikon D850 - Sigma ART 50mm f/1.4 DG HSM - f/11, 0.8s, ISO 80.

870
871
872
873
874
875
876

877

878

879

880

881

	Type of approaches and associated processing	Average completion time		Ease of implementation	Cost	Advantages	Disadvantages
		Acquisition	Processing				
2D	Drawing + Layout	Highly variable - Moderate		Difficult - Requires training	Low	Very low cost - No specialized equipment required	Time-consuming and challenging - Subject to interpretation but can be precise if well executed - Quality varies depending on the illustrator
	Traditional Photography + Photoshop	Fast	Fast	Accessible	Moderate	Mobile equipment - Speed - Visualization of color/texture	Often incomplete and interpretative - Difficult for technological analysis - Does not provide surface topography information - No quantitative data - Optical distortion
	Focus Stacking Photography	Fast to moderate	Moderate (precise)	Accessible	Moderate	Mobile equipment - Increases depth of field and sharpness - Enables high-resolution fine detail - Useful for macrophotography	Sensitive to subject or camera movement (can easily generate artifacts) - Does not provide surface topography information - No quantitative data - Optical distortion
2D ^{1/2}	RTI + Relight, RTI Viewer, and Photoshop	Fast to moderate		Accessible	Moderate	Fast and simple acquisition and processing - Mobile equipment - Objective and precise visualization of micro-reliefs (often invisible to the naked eye) - Facilitates technological analysis	Large final file size - Optical distortion
3D	3D Scan - MicroCT Scan	Fast to moderate		Moderate to difficult - Requires training	High	3D model - Batch acquisition of pieces	High cost - Equipment is difficult if not impossible to move - Large final file size
	Photogrammetry	Fast to moderate	Long	Moderate - Requires training	Moderate	3D model - Lower cost compared to scanning - Mobile equipment	Long processing time - Large final file size - Lacks precision in fine details - Difficult technological analysis

882
883
884

Table 1 - Summary table of the different criteria to consider when choosing a type of lithic illustration (non-exhaustive)

Acknowledgements

886 We would like to express our gratitude to the Musée National de Préhistoire des Eyzies,
887 particularly its director, Nathalie Fourment, for granting access to its collections, which
888 enabled the acquisition of new photographs, RTI images, and 3D models of selected
889 pieces. We also thank the Nouvelle Aquitaine research project “ADNER” (*Apprendre*
890 *Différemment avec les Néandertaliens récents: humanités passées, humanités croisées au*
891 *cœur de l’innovation scientifique, pédagogique et culturelle* – AAPR2021-2020-11779310;
892 2021-26) for funding the Master’s thesis (J. Looten) directed by J.-G. Bordes and B.
893 Gravina. The RTI images and photographs of lithic artifacts from Grotte XVI (Dordogne,
894 France) were produced for this project, which also forms the basis of this article. Special
895 thanks to Agnès Lamotte (HALMA – UMR 8164) for authorizing the use of diacritical
896 sketches created as part of Julien Looten’s doctoral research thesis. We also thank
897 Dominique Cliquet for permitting the use of RTI images from the project “*Les premiers*
898 *peuplements de Normandie*” (Cliquet, dir.; 2024), carried out by J. Looten. Finally, we
899 extend our gratitude to Jacques Jaubert, Gauthier Devilder, Nelson Ahmed-Delacroix, and
900 Celia Fatcheung, the illustrators who generously shared their expertise on the challenges
901 and time required for creating stone tool drawings.

902

903

904

905

906

907

908

909

910

911

912

913

914

915

916

917

918

919

920

921

922

923

924

925

926

927

928

929

930

933 ADDINGTON L.R. (1986) – *Lithic illustration: drawing flaked stone artifacts for publication*,
934 Chicago : University of Chicago Press, 270 p.

936 AIRVAUX J., (2005) – Note sur de nouveaux procédés pour le dessin des objets lithiques,
937 *Bulletin Préhistoire du Sud-Ouest*, 12, 2, p. 218-221.

939 ASSIÉ Y. (1995) – Dessin de l'industrie lithique préhistorique. Notions élémentaires et
940 conseils pratiques. *Préhistoire Anthropologie Méditerranéennes*, 4, p. 191-227.

942 BARONE S., NERI P., PAOLI A., RAZIONALE A.V. (2018) – Automatic technical
943 documentation of lithic artefacts by digital techniques, *Digital Applications in*
944 *Archaeology and Cultural Heritage*, 11, p. e00087. DOI:
945 <https://doi.org/10.1016/j.daach.2018.e00087>

947 BORDES F. (1953) – Essai de classification des industries « moustériennes », *BSPF*, 50,
948 7-8, p. 457-466.

950 BORDES F. (1984) – *Leçons sur le Paléolithique, Tome 2 : Le Paléolithique en Europe*.
951 Paris : Éditions du Centre National de la Recherche Scientifique (CNRS), 462 p.

953 BRECKO J., MATHYS A., DEKONINCK W., LEPONCE M., VANDENSPIEGEL D., SEMAL
954 P. (2014) – Focus stacking: Comparing commercial top-end set-ups with a semi-
955 automatic low budget approach. A possible solution for mass digitization of type
956 specimens, *ZooKeys*, 464, p. 1-23. DOI: [10.3897/zookeys.464.8615](https://doi.org/10.3897/zookeys.464.8615)

958 BRECKO J., MATHYS A. (2020) – Handbook of best practice and standards for 2D+ and
959 3D imaging of natural history collections, *European Journal of Taxonomy*, 623, p. 1-115.
960 DOI: <https://doi.org/10.5852/ejt.2020.623>

962 BULLENKAMP J.P., LINSEL F., MARA H. (2022) – Lithic Feature Identification in 3D based
963 on Discrete Morse Theory. In: *Eurographics Workshop on Graphics and Cultural*
964 *Heritage*, ed. By Ponchio F and Pintus R., The Eurographics Association, p. 55-58.
965 DOI: [10.2312/gch.20221224](https://doi.org/10.2312/gch.20221224)

967 BUSTOS-PÉREZ G., GRAVINA B., BRENET M., ROMAGNOLI F. (2024) – The
968 Contribution of 2D and 3D Geometric Morphometrics to Lithic Taxonomies: Testing
969 Discrete Categories of Backed Flakes from Recurrent Centripetal Core Reduction,
970 *Journal of Paleolithic Archaeology*, 7, 5, 23 p. DOI: [10.1007/s41982-023-00167-7](https://doi.org/10.1007/s41982-023-00167-7)

972 CAUX S., GALLAND A., QUEFFELEC A., BORDES J.-G. (2018) – Aspects and
973 characterization of chert alteration in an archaeological context: A qualitative to
974 quantitative pilot study, *Journal of Archaeological Science: Reports*, 20, p. 210-219.
975 DOI: <https://doi.org/10.1016/j.jasrep.2018.04.027>

977 CAUCHE D. (2020) – Le dessin scientifique des outils lithiques préhistoriques et ses
978 normes. Exemple des collections de la grotte de l'Observatoire (Monaco), *Bulletin du*
979 *Musée d'Anthropologie préhistorique de Monaco*, n°59, p. 29-40.

981 CERASONI J.N. (2021) - Vectorial application for the illustration of archaeological lithic
982 artefacts using the “Stone Tools Illustrations with Vector Art” (STIVA) Method. *PLOS*
983 *ONE* ,16(5): e0251466. DOI: <https://doi.org/10.1371/journal.pone.0251466>
984

985 CHAPMAN, K., PETERSON, J.R., CROSS, A., (2017) - Reflectance transformation
986 imaging (rti): Capturing gravestone detail via multiple digital images. *Association for*
987 *Gravestone Studies* 42 (2).
988

989 CONRAD O., BECHTEL B., BOCK M., DIETRICH H., FISCHER E., GERLITZ L.,
990 WEHBERG J., WICHMANN V., BÖHNER J. (2015) – System for Automated
991 Geoscientific Analyses (SAGA) v. 2.1.4, *Geoscientific Model Development Discussions*,
992 8, p. 2271-2312. DOI: [10.5194/gmdd-8-2271-2015](https://doi.org/10.5194/gmdd-8-2271-2015)
993

994 COSENTINO, A. (2013) - Macro photography for reflectance transformation imaging: A
995 practical guide to the highlights method. *E-conserv.* J. 1.
996

997 CULTURAL HERITAGE IMAGING. (2010) – *Reflectance Transformation Imaging. Guide to*
998 *Highlight Image Capture*, Cultural Heritage, San Francisco, 26 p.
999

1000 CULTURAL HERITAGE IMAGING. (2013) – *Reflectance Transformation Imaging. Guide to*
1001 *RTIViewer. Version 1.1*. Cultural Heritage Imaging and Visual Computing Lab, ISTI-
1002 Italian National Research Council, San Francisco. [URL :
1003 [https://culturalheritageimaging.org/What_We_Offer/Downloads/rtiviewer/](https://culturalheritageimaging.org/What_We_Offer/Downloads/rtiviewer/RTIViewer_Guide_v1_1.pdf)
1004 [RTIViewer_Guide_v1_1.pdf](https://culturalheritageimaging.org/What_We_Offer/Downloads/rtiviewer/RTIViewer_Guide_v1_1.pdf) consulted on 02/16/2025]
1005

1006 CULTURAL HERITAGE IMAGING. (2018) – *Multilight Imaging - Highlight-Reflectance*
1007 *Transformation Imaging (H-RTI) for Cultural Heritage*, Historic England, 72 p.
1008

1009 DAUVOIS M. (1976) – *Précis de dessin dynamique et structural des industries lithiques*
1010 *préhistoriques*. Fanlac, Périgueux, 262 p.
1011

1012 DELPIANO D., COCILOVA A., ZANGROSSI F., PERESANI M. (2019) – Potentialities of
1013 the virtual analysis of lithic refitting: case studies from the Middle and Upper Paleolithic,
1014 *Archaeological and Anthropological Sciences*, 11, p. 4467-4489. DOI: [10.1007/s12520-](https://doi.org/10.1007/s12520-019-00779-7)
1015 [019-00779-7](https://doi.org/10.1007/s12520-019-00779-7)
1016

1017 DEMARS P.-Y., LAURENT P. (1989) – *Types d’outils lithiques du Paléolithique supérieur*
1018 *en Europe*, Paris, CNRS ed., 178 p.
1019

1020 DER APRAHAMIAN G., ET ABBES F. (2015) – Le dessin d’objets lithiques, ArchéOrient –
1021 Le Blog [URL : <https://archeorient.hypotheses.org/4170> consulted on 02/16/2025]. DOI :
1022 <https://doi.org/10.58079/bctu>
1023

1024 DESMOND A., CARTWRIGHT I., ALLEN R. (2021) – Documenting Functional Use-Wear
1025 on Bone Tools: An RTI Approach. *J. Comp. Appl. Archaeol.*, 4(1), 214–229. DOI :
1026 <https://doi.org/10.5334/jcaa.80>
1027

1028 DI MAIDA G., HATTERMANN M., DELPIANO D. (2023) – 3D models of lithic artefacts: A
1029 test on their efficacy, *Digital Applications in Archaeology and Cultural Heritage*, 30. DOI:
1030 <https://doi.org/10.1016/j.daach.2023.e00279>
1031

- 1032 DIAZ-GUARDAMINO M., WHEATLEY D. (2013) – Rock art and digital technologies: The
1033 application of Reflectance Transformation Imaging (RTI) and 3D laser scanning to the
1034 study of Late Bronze Age Iberian stelae, *MENGA. Journal of Andalusian Prehistory*, 4,
1035 p. 187-203.
1036
- 1037 EARL G., BEALE G., MARTINEZ K., PAGI H. (2010a) - Polynomial texture mapping and
1038 related imaging technologies for the recording, analysis and presentation of
1039 archaeological materials, In: Mills, J.P., Barber, D.M., Miller, P.E., Newton, I. (Eds.),
1040 *Proceedings of the ISPRS Commission V Mid-Term Symposium 'Close Range Image*
1041 *Measurement Techniques'*, *ISPRS 38(5)*. Newcastle upon Tyne, UK, pp. 218–223.
1042
- 1043 EARL G., MARTINEZ K., MALZBENDER T. (2010b) – Archaeological applications of
1044 polynomial texture mapping: analysis, conservation and representation, *Journal of*
1045 *Archaeological Science*, 37, 8, p. 2040-2050. DOI:
1046 <https://doi.org/10.1016/j.jas.2010.03.009>
1047
- 1048 EARL G., BASFORD P., BISCHOFF A., BOWMAN A.R., CROWTHER C., DAHL J.,
1049 HODGSON M., ISAKSEN L., KOTOULA E., MARTINEZ K., PAGI H., PIQUETTE K.E.
1050 (2011) – Reflectance Transformation Imaging Systems for Ancient Documentary
1051 Artefacts. In: Bowen, J.P., Dunn, S., Kia, Ng (Eds.), EVA. London 2011: *Electronic*
1052 *Visualization and the Arts*. BCS, London, p. 147–154. DOI: [10.14236/ewic/EVA2011.27](https://doi.org/10.14236/ewic/EVA2011.27)
1053
- 1054 EVANS J. (1872) – *The ancient stone implements, weapons, and ornaments, of Great*
1055 *Britain*, London : Longmans, Green, Reader, and Dyer, 672 p.
1056
- 1057 FIORINI A. (2018) – Il metodo fotografico RTI (Reflectance Transformation Imaging) per la
1058 documentazione delle superfici archeologiche : L'applicazione ai materiali di età
1059 protostorica, *Archeologia e Calcolatori*, 29, p. 241-258. DOI:
1060 <https://doi.org/10.19282/ac.29.2018.20>
1061
- 1062 FORSTER-HEINLEIN B., VAN DE VILLE D., BERENT J., SAGE D., UNSER M. (2004) –
1063 Complex wavelets for extended depth-of-field: A new method for the fusion of
1064 multichannel microscopy images, *Microscopy research and technique*, 65, p. 33-42.
1065 DOI: <https://doi.org/10.1002/jemt.20092>
1066
- 1067 FRERE J. (1800) – Account of Flint Weapons Discovered at Hoxne in Suffolk.
1068 *Archaeologia*, vol. 13, 1800, p. 204-205.
1069
- 1070 GARCÍA-MEDRANO P., MALDONADO-GARRIDO E., ASHTON N., OLLE A. (2020) –
1071 Objectifying processes: The use of geometric morphometrics and multivariate analyses
1072 on Acheulean tools, *Journal of Lithic Studies*, 7, 1, 16 p. DOI:
1073 <https://doi.org/10.2218/jls.4327>
1074
- 1075 GOLDMAN Y., LINN R., SHAMIR O., WEINSTEIN-EVRON M. (2018) – Micro-RTI as a
1076 novel technology for the investigation and documentation of archaeological textiles,
1077 *Journal of Archaeological Science: Reports*, 19, p. 1-10. DOI:
1078 [10.1016/J.JASREP.2018.02.013](https://doi.org/10.1016/J.JASREP.2018.02.013)
1079
- 1080 GRIWODZ C., GASPARINI S., CALVET L., GURDJOS P., CASTAN F., MAUJEAN B., DE
1081 LILLO G., LANTHONY Y. (2021) – AliceVision Meshroom: An open-source 3D
1082 reconstruction pipeline, In: *Proceedings of the 12th ACM Multimedia Systems*

1083 Conference, New York, NY, USA, Association for Computing Machinery (MMSys '21),
1084 p. 241-247. DOI: <https://doi.org/10.1145/3458305.3478443>
1085

1086 HAMMER O., BENGTON S., MALZBENDER T., GELB D. (2002) – Imaging fossils using
1087 reflectance transformation and interactive manipulation of virtual light sources,
1088 *Palaeontol. Electronica*, 5, 1, p.1-9.
1089

1090 HERZLINGER G., GOREN-INBAR N., GROSMAN L. (2017) – A new method for 3D
1091 geometric morphometric shape analysis: The case study of handaxe knapping skill,
1092 *Journal of Archaeological Science: Reports*, 14, p. 163-173. DOI:
1093 <https://doi.org/10.1016/j.jasrep.2017.05.013>
1094

1095 HERZLINGER G., GROSMAN L. (2018) – AGMT3-D: A software for 3-D landmarks-based
1096 geometric morphometric shape analysis of archaeological artifacts, *PLOS ONE*, 13, 11,
1097 e0207890. DOI: <https://doi.org/10.1371/journal.pone.0207890>
1098

1099 HORN C., LING J., BERTILSSON U., POTTER R. (2018) – By All Means Necessary –
1100 2.5D and 3D Recording of Surfaces in the Study of Southern Scandinavian Rock Art,
1101 *Open Archaeology*, 4, 1, p. 81-96. DOI : <https://doi.org/10.1515/opar-2018-0005>
1102

1103 HUGHES-HALLETT M., YOUNG C., MESSIER P. (2021) – A Review of RTI and an
1104 Investigation into the Applicability of Micro-RTI as a Tool for the Documentation and
1105 Conservation of Modern and Contemporary Paintings, *Journal of the American Institute*
1106 *for Conservation*, 60, 1, p. 18-31. DOI: <https://doi.org/10.1080/01971360.2019.1700724>
1107

1108 INIZAN M.-L., REDURON M., ROCHE H., TIXIER J. (1995) – *Technologie de la pierre*
1109 *taillée*. Cercle de Recherche et d'Etudes Préhistoriques, Meudon, 200 p
1110

1111 KOSCIUK J., TELESIŃSKA M., NISZTUK M., PAKOWSKA M. (2020) – Documentation of
1112 the most important petroglyphs by structured light scanning and analysis of the most
1113 damaged petroglyphs by vPTM and vRTI methods, *Architectus*, 2 (62), p. 44-57.
1114 DOI: [10.37190/arc200207](https://doi.org/10.37190/arc200207)
1115

1116 KOTOULA E. & EARL G. (2015) - Integrated RTI approaches for the study of painted
1117 surfaces. In *CAA 2014, Archaeopress*, pp. 123–134.
1118

1119 LAMOTTE A. & MASSON E. (2016) – Arché-OBIA : un concept d'analyse quantitative
1120 d'images numériques appliqué aux bifaces du gisement de Gouzeaucourt (Nord). *Notae*
1121 *prehistoricae*, n°36, p. 121-130.
1122

1123 LAURENT P. (1985) – Le dessin des objets préhistoriques : une introduction / Drawing of
1124 prehistoric implements : an introduction, *Revue archéologique du Centre de la France*,
1125 24, 1, p. 83-96.
1126

1127 LOWE D.G. (2004) – Distinctive Image Features from Scale-Invariant Keypoints,
1128 *International Journal of Computer Vision*, 60, 2, p. 91-110. DOI:
1129 <https://doi.org/10.1023/B:VISI.0000029664.99615.94>
1130

1131 LUHMANN, T., ROBSON, S., KYLE, S., & BOEHM, J. (2019) – *Close-Range*
1132 *Photogrammetry and 3D Imaging*. Berlin, Boston : De Gruyter. DOI:
1133 <https://doi.org/10.1515/9783110607253>.

1134
1135 LYCETT S.J., CRAMON-TAUBADEL N. VON, GOWLETT J.A.J. (2010) – A comparative
1136 3D geometric morphometric analysis of Victoria West cores: implications for the origins
1137 of Levallois technology, *Journal of Archaeological Science*, 37, 5, p. 1110-1117. DOI:
1138 <https://doi.org/10.1016/j.jas.2009.12.011>
1139
1140 LYMER K. (2015) – Image processing and visualisation of rock art laser scans from
1141 Loups's Hill, County Durham, *Digital Applications in Archaeology and Cultural Heritage*,
1142 2, 2-3, p. 155-165. DOI: <http://dx.doi.org/10.1016/j.daach.2015.01.002>
1143
1144 MAGNANI, M. (2014) – Three-Dimensional Alternatives to Lithic Illustration, *Advances in*
1145 *Archaeological Practice*, 2, 4, p. 285-297. DOI: [https://doi.org/10.7183/2326-](https://doi.org/10.7183/2326-3768.2.4.285)
1146 [3768.2.4.285](https://doi.org/10.7183/2326-3768.2.4.285).
1147
1148 MALZBENDER T., GELB D., WOLTERS H. (2001) – Polynomial texture maps, *In:*
1149 *Proceedings of the 28th annual conference on Computer graphics and interactive*
1150 *techniques*, ACM SIGGRAPH, Los Angeles, August 12-17, 2001, p. 519-528. DOI:
1151 <https://doi.org/10.1145/383259.383320>
1152
1153 MARTINGELL, H., & SAVILLE, A. (1988) – *The Illustration of Lithic Artefacts: A Guide to*
1154 *Drawing Stone Tools for Specialist Reports*. Association of Archaeological Illustrators &
1155 Surveyors et Lithic Studies Society.
1156
1157 MASSON MOUREY J. (2019) – First application of Reflectance Transformation Imaging
1158 (RTI) on Prehistoric Rock Engravings of the Monte Bego Region (Tende, Alpes-
1159 Maritimes, France), *INORA*, 84, p. 24-30.
1160
1161 MATHYS, A., BRECKO, J., & SEMAL, P. (2013) – Comparing 3D digitizing technologies:
1162 What are the differences? *In: Digital Heritage International Congress, 2013*, 1-8. DOI:
1163 <https://doi.org/10.1109/DigitalHeritage.2013.6743733>.
1164
1165 MEDINA, J.J., MALEY, J.M., SANNAPAREDDY, S., MEDINA, N.N., GILMAN, C.M., &
1166 MCCORMACK, J.E. (2020) – A rapid and cost-effective pipeline for digitization of
1167 museum specimens with 3D photogrammetry. *PLoS ONE*, 15, 8, e0236417. DOI:
1168 <https://doi.org/10.1371/journal.pone.0236417>.
1169
1170 MORRONE A., PAGI H., TÖRV M., ORAS E. (2019) – Application of Reflectance
1171 Transformation Imaging (RTI) to surface bone changes in paleopathology,
1172 *Anthropologischer Anzeiger*, 53, p. 295-315. DOI: [10.1127/anthranz/2021/1315](https://doi.org/10.1127/anthranz/2021/1315)
1173
1174 MUDGE M., VOUTAZ J.-P., SCHROER C., LUM M. (2005) – Reflection Transformation
1175 Imaging and Virtual Representations of Coins from the Hospice of the Grand St.
1176 Bernard., *In: Mudge, M., Ryan, N., Scopigno, R. (Eds.), Proceedings of the 6th*
1177 *International Symposium on Virtual Reality, Archaeology and Cultural Heritage*
1178 (VAST2005) p. 29-39. DOI: [10.2312/VAST/VAST05/029-039](https://doi.org/10.2312/VAST/VAST05/029-039)
1179
1180 MUDGE M., MALZBENDER T., SCHROER C., LUM M. (2006) – New Reflection
1181 Transformation Imaging Methods for Rock Art and Multiple-Viewpoint Display, *In:*
1182 *Ioannides, M., Arnold, D., Niccolucci, F., Mania, K. (Eds.), Proceedings of the 7th*
1183 *International Symposium on Virtual Reality, Archaeology and Cultural Heritage*
1184 (VAST2006), p. 195-202. DOI: [10.2312/VAST/VAST06/195-202](https://doi.org/10.2312/VAST/VAST06/195-202)

1185
1186 MUDGE M., MALZBENDER T., CHALMERS A., SCOPIGNO R., DAVIS J., WANG O.,
1187 GUNAWARDANE P., ASHLEY M., DOERR M., PROENCA A., BARBOSA J. (2008) –
1188 Image-Based Empirical Information Acquisition, Scientific Reliability, and Long-Term
1189 Digital Preservation for the Natural Sciences and Cultural Heritage, *EUROGRAPHICS*,
1190 30 p.
1191
1192 NEWMAN S.E. (2015) – Applications of Reflectance Transformation Imaging (RTI) to the
1193 study of bone surface modifications, *Journal of Archaeological Science*, 53, p. 536-549.
1194 DOI: <https://doi.org/10.1016/j.jas.2014.11.019>
1195
1196 PAWLOWICZ, D. (2015) – *Reflectance Transformation Imaging for Lithics* – Website URL :
1197 <https://rtimage.us/> consulted on 02/16/2025.
1198
1199 PELEGRIN J. (2000) – Les techniques de débitage laminaire au Tardiglaciaire: critères de
1200 diagnose et quelques réflexions., *In* : Valentin B., Bodu p., Cristensen M. (dir.), *L'Europe*
1201 *Centrale et Septentrionale au Tardiglaciaire: confrontation des modèles régionaux de*
1202 *peuplement*, Actes de la Table ronde (Nemours 13-16 Mai 1997), APRAIF, 7, p. 73-86.
1203
1204 PONCHIO F., CORSINI M., SCOPIGNO R. (2019) – RELIGHT: a compact and accurate
1205 RTI representation for the Web, *Graphical Models*, 105, p. 101040.
1206 DOI: [10.1016/j.gmod.2019.101040](https://doi.org/10.1016/j.gmod.2019.101040)
1207
1208 PORTER S.T., HUBER N., HOYER C., FLOSS H. (2016) – Portable and low-cost solutions
1209 to the imaging of Paleolithic art objects: A comparison of photogrammetry and
1210 reflectance transformation imaging, *Journal of Archaeological Science: Reports*, 10, p.
1211 859-863. DOI: <https://doi.org/10.1016/j.jasrep.2016.07.013>
1212
1213 PULLA S., RAZDAN A., FARIN G. (2001) – Improved Curvature Estimation for Watershed
1214 Segmentation of 3-Dimensional Meshes, *IEEE Transactions on Visualization and*
1215 *Computer Graphics*, 7, p. 1-15
1216
1217 PURDY B.A., JONES K.S., MECHOLSKY J.J., BOURNE G., HULBERT R.C.,
1218 MACFADDEN B.J., CHURCH K.L., WARREN M.W., JORSTAD T.F., STANFORD D.J.,
1219 WACHOWIAK M.J., SPEAKMAN R.J. (2011) – Earliest art in the Americas: incised
1220 image of a proboscidean on a mineralized extinct animal bone from Vero Beach,
1221 Florida, *Journal of Archaeological Science*, 38, 11, p. 2908-2913. DOI:
1222 <https://doi.org/10.1016/j.jas.2011.05.022>
1223
1224 RICHARDSON, E., GROSMAN, L., SMILANSKY, U., & WERMAN, M. (2014) – Extracting
1225 scar and ridge features from 3D-scanned lithic artifacts. *In*: E. Earl, T. Sly, D. Wheatley,
1226 I. Romanowska, K. Papadopoulos, P. Murrieta-Flores, & A. Chrysanthi (Eds.),
1227 *Archaeology in the Digital Era*, Amsterdam: Amsterdam University Press, p. 83-92. DOI:
1228 <https://doi.org/10.2307/j.ctt6wp7kg.12>
1229
1230 ROBITAILLE, J. (2025) - Reflectance Transformation Imaging at a Microscopic Level: A
1231 New Device and Method for Collaborative Research on Artifact Use-Wear Analysis.
1232 *Journal of Archaeological Science: Reports*, 61, 104914.
1233 DOI : <https://doi.org/10.1016/j.jasrep.2024.104914>
1234
1235

- 1236 ROBITAILLE J., MEYERING L.-E., GAUDZINSKI-WINDHEUSER S., PETTITT P., JÖRIS
1237 O., KENTRIDGE R. (2024) – Upper Palaeolithic fishing techniques: Insights from the
1238 engraved plaquettes of the Magdalenian site of Gönnersdorf, Germany, *PLOS ONE*, 19,
1239 11, p. e0311302. DOI : <https://doi.org/10.1371/journal.pone.0311302>
1240
- 1241 ROCHEBRUNE, A.-T. DE. (1881) – *Les Troglodytes de La Gartempe. Fouilles de la grotte*
1242 *des Cottés*. Paris : Imprimerie Nationale. 126 p.
1243
- 1244 SCHÖNBERGER, J., & FRAHM, J.-M. (2016) – *Structure-from-Motion Revisited*. In:
1245 *Proceedings of the IEEE Conference on Computer Vision and Pattern Recognition*
1246 *(CVPR)*. p. 4104-4113. DOI: <https://doi.org/10.1109/CVPR.2016.445>
1247
- 1248 SMITH H., JENNINGS T., SMALLWOOD A. (2024) – The third dimension of stone points:
1249 2D vs. 3D geometric morphometric shape analysis, *Archaeological and Anthropological*
1250 *Sciences*, 16, 170, DOI: [10.1007/s12520-024-02069-3](https://doi.org/10.1007/s12520-024-02069-3)
1251
- 1252 SONNEVILLE-BORDES, D. DE. (1960) – *Le Paléolithique supérieur en Périgord* (Thèse -
1253 *Sciences*). Delmas, Bordeaux. 580 p.
1254
- 1255 TAKAKURA J. (2020) – Rethinking the Disappearance of Microblade Technology in the
1256 Terminal Pleistocene of Hokkaido, Northern Japan: Looking at Archaeological and
1257 Palaeoenvironmental Evidence, *Quaternary*, 3, p. 21. DOI: [10.3390/quat3030021](https://doi.org/10.3390/quat3030021)
1258
- 1259 TARINI, M., CIGNONI, P., & MONTANI, C. (2006) – Ambient Occlusion and Edge Cueing
1260 to Enhance Real Time Molecular Visualization. *IEEE Transactions on Visualization and*
1261 *Computer Graphics*, 12, 5, p. 1237-1244. DOI: [10.1109/TVCG.2006.115](https://doi.org/10.1109/TVCG.2006.115)
1262
- 1263 TIMBRELL, L. (2022) - A Collaborative Model for Lithic Shape Digitization in Museum
1264 Settings. *Lithic Technology*, 48(1), 31–42.
1265 DOI: <https://doi.org/10.1080/01977261.2022.2092299>
1266
- 1267 VILA A. (2017) – *Mise en place d'une procédure de calibration pour un dispositif*
1268 *d'acquisition dédié aux techniques de Reflectance Transformation Imaging*, École
1269 Nationale Supérieure Louis Lumière, Saint-Denis (France), Master's thesis, 100 p.